Journal Pre-proof

Solar forcing for nutricline depth variability inferred by coccoliths in the pre-industrial northwestern Mediterranean

Alessandro Incarbona, Sergio Bonomo, Isabel Cacho, Fabrizio Lirer, Giulia Margaritelli, Delia Pecoraro, Patrizia Ziveri

PII: S0921-8181(23)00075-9

DOI: https://doi.org/10.1016/j.gloplacha.2023.104102

Reference: GLOBAL 104102

To appear in: *Global and Planetary Change*

Received date: 7 November 2022

Revised date: 4 March 2023

Accepted date: 24 March 2023

Please cite this article as: A. Incarbona, S. Bonomo, I. Cacho, et al., Solar forcing for nutricline depth variability inferred by coccoliths in the pre-industrial northwestern Mediterranean, *Global and Planetary Change* (2023), https://doi.org/10.1016/j.gloplacha.2023.104102

This is a PDF file of an article that has undergone enhancements after acceptance, such as the addition of a cover page and metadata, and formatting for readability, but it is not yet the definitive version of record. This version will undergo additional copyediting, typesetting and review before it is published in its final form, but we are providing this version to give early visibility of the article. Please note that, during the production process, errors may be discovered which could affect the content, and all legal disclaimers that apply to the journal pertain.

© 2023 Published by Elsevier B.V.

Solar Forcing for Nutricline Depth variability inferred by Coccoliths in the Pre-Industrial Northwestern Mediterranean

Alessandro Incarbona[1,2*], Sergio Bonomo[3], Isabel Cacho[4], Fabrizio Lirer[5,3], Giulia Margaritelli[6], Delia Pecoraro[1], Patrizia Ziveri[7,8]

[1]Università degli Studi di Palermo, Dipartimento di Scienze della Terra e del Mare, Via Archirafi 22, 90134 Palermo, Italy.
[2]National Biodiversity Future Center (NBFC), Piazza Marina 61, Palermo 90133, Italy.
[3]Istituto di Geologia Ambientale e Geoingegneria (CNR-IGAG), Area Della Ricerca di Roma 1- Strada Provinciale 35d, Montelibretti, 9-00010, RM, Italy
[4]GRC Geociències Marines, Dept. de Dinàmica de la Terra i de l'Oceà, Facultat de Ciències de la Terra, Universitat de Barcelona, Barcelona, 08028, Spain
[5]Sapienza Università di Roma, Dipartimento di Scienze della Terra, Piazzale A. Moro 5, Roma, 00185, Italy
[6]Istituto di Ricerca per la Protezione Idrogeologica (IRPI), CNR, Via Madonna Alta 126, Perugia, 06128, Italy
[7]Universitat Autònoma de Barcelona (UAB), Institute of Environmental Science and Technology (ICTA), Edifici Z, Carrer de les Columnes, Campus de la UAB, 08193 Bellaterra (Cerdanyola del Vallès), Barcelona, Spain
[8] Catalan Institution for Research and Advanced Studies (ICREA), 08010, Barcelona, Spain

*Corresponding Author e-mail, alessandro.incarbona@unipa.it; telephone, +39 091 23864648.

Journal Pre-proof

Abstract

The oceanic system has been rapidly changing under human-induced climate change that is taking place at unprecedented rates. The paleoclimate archive of the last two millennia is often adopted to discern the ongoing anthropogenic global warming from the pre-industrial natural climate variability. the Mediterranean Sea is an especially critical system, being particularly affected by climate change. A common group of marine unicellular planktonic calcifiers, coccolithophores, are forming calcite plates, coccoliths. When reaching the sediments, they have been employed as a proxy in many paleoenvironmental reconstructions and are

increasingly used in the last centuries. Recent studies indicate a subtle response to historical climate changes, except for primary productivity switches during the Little Ice Age and, most importantly, across the Industrial age.

In this work, we use coccolith decadal-scale resolution data from core HER-MC-MR3.3, recovered in the Balearic Sea, exploring their variability over the pre-industrial age, from 700 BCE to 1740 CE. Results are compared to planktonic foraminifera stable isotopes, planktonic foraminiferal assemblages, alkenone-derived SSTs and foraminiferal Mg/Ca-derived SSTs, previously acquired in the same sediment core. Abundance variations in coccolith assemblages, expressed as Shannon-Wiener diversity H-index changes or as trends and fluctuations in ecological groups are associated with historical climate changes, among others the Medieval Climatic Anomaly and the Little Ice Age, indicating repeated modifications in surface water conditions, in response to hydrological and atmospheric changing patterns. A tight relationship between deep nutricline and upper water column stratified conditions, derived from high abundance of *Florisphaera profunda*, and high solar irradiation levels is established. The solar activity fingerprint in the *F. profunda* distribution pattern is further assessed by spectral analysis, with the emergence of significant periodicities observed in solar activity proxies, among others the well known de Vries-Suess cycle. Finally, we notice small but statistically significant abundance fluctuations in holococcoliths (solution susceptible coccolith forms) that may be tied to their enhanced preservation during increased rainfall in western Europe. This implies the advection of westerlies and long-lasting blocking events that may have promoted deep-water formation and seafloor ventilation during this time. The comparison with sedimentological proxies of bottom current strength shows some inconsistencies but still defines variable and intermittent deep-water formation rates in the Gulf of Lions over the pre-industrial period.

1 – Introduction

Greenhouse gases emission from human activity since the second industrial revolution (1857 Common Era – CE) led to monthly average CO_2 and CH_4 atmospheric levels of respectively ~420 ppm and ~1900 ppb (https://gml.noaa.gov/ccgg/trends/; https://www.esrl.noaa.gov/gmd/ccgg/trends_ch4/), whose values are much higher than the highest ones recorded in the Antarctica ice cores over the last 800 kiloyears and the last nine glacial/interglacial cycles (Loulergue et al., 2008; Lüthi et al., 2008; Siegenthaler et al., 2015). The global temperature (0.8-1.2°C) and sea-level (20 cm) rise took place at unprecedented

rates and are thought to be especially harmful in the Mediterranean Sea, an important climate change hotspot region (Lionello et al., 2006; MedECC, 2021).

A two thousand years (2k) time window is often paralleled to discern the human-induced climate change from the natural climatic variability and trend. The pre-industrial worldwide Sea Surface Temperature (SST) was gently declining, likely due to sunspot minimum activity and explosive volcanism (McGregor et al., 2015). Different climatic phases in the Middle-Late Holocene (e.g. Little Ice Age, Medieval Climatic Anomaly, Roman period) have been identified by historical documentation and paleoclimatic proxies and their influence on ancient civilization rise and fall is well-established (e.g. Büntgen et al., 2016; Drake, 2012; Hodell et al., 2001; Margaritelli et al., 2020a). Their better understanding, in terms of impact of climatic forcing on terrestrial and marine paleoenvironments, mechanisms and processes in place, is still a basic requisite to manage natural hazards related to the ongoing climate change. Over the last 2700 years of the studied record, we identify five climatic periods, whose duration follows Büntgen et al. (2016), Margaritelli et al. (2018) and Lenkom et al. (2019): Talaiotic period (TP) base of the record – 0 CE (correspond to the Bronze Age in Margaritelli et al., 2018); Roman warm period (RP) 0-400 CE; Dark Age (400-800 CE), which includes a short Late Antique Little Ice Age between 540 and 660 CE (Büntgen et al., 2016); Medieval Climate Anomaly (MCA) 800-1250 CE; Little Ice Age (LIA) 1250-1850 CE.

Coccolithophores are golden-brown unicellular planktonic algae, with calcite plates, the so-called coccoliths, that are dispersed on the seafloor after their sinking. Living coccolithophores play a key role in today's ocean in regulating carbonate chemistry and CO_2 atmospheric levels (Ziveri et al., 2023). Coccoliths are employed in a large set of paleoenvironmental and paleoceanographic reconstructions (Baumann et al., 2005) and in the Mediterranean Sea show a ready response to abrupt climate changes, such as Dansgaard-Oeschger events or Holocene rapid climatic changes, mainly in terms of primary productivity variability and vertical water column dynamics (Ausín et al., 2015; Bazzicalupo et al., 2018, 2020; Cascella et al., 2021; Colmenero-Hidalgo et al., 2004; Di Stefano et al., 2015; Flores et al., 1997; Incarbona et al., 2008, 2013, 2019a; Triantaphyllou, 2014; Triantaphyllou et al., 2009a). More subtle seems to be the response to historical climate changes, generally lacking any sign of significant abundance variation or expressed like just general trends (Bonomo et al., 2016; Cascella et al., 2019; Vallefuoco et al., 2012), though primary productivity changes have been inferred during the Little Ice Age (Incarbona et al., 2010a) and, most importantly, for the first time, across the Industrial age (Pallacks et al., 2021). The shortage of robust evidence of coccolithophore changes contrasts with more evident variability found in planktonic foraminiferal assemblages

(Incarbona et al., 2019b; Lirer et al., 2014; Margaritelli et al., 2016, 2018; Margaritelli al., 2020b; Pallacks et al., 2021; Vallefuoco et al., 2012). However, this difference may be tied to the lower number of coccolith studies and to less sensitive oceanographic settings.
Here we explore the variability of pre-industrial (from 700 BCE to 1740 CE) coccolith assemblages in sediments of core HER-MC-MR3.3 (thereafter MR3.3) recovered in the Balearic Sea. Previous data acquired on the MR3.3 core deal with alkenone-derived and Mg/Ca SST, planktonic foraminiferal assemblages, multi-species planktonic foraminiferal stable isotopes and sediment grain size parameters (Cisneros et al., 2019, 2016; Margaritelli et al., 2018). We show that significant abundance variations and/or trends in coccolith assemblages are associated with historical climate changes, indicating repeated modifications in surface water conditions, in response to hydrological and atmospheric changing patterns.

2- Material and Methods

2.1 - Material

The MR3.3 27-cm long multicore was recovered in the deep-water Minorca sediment drift (40°29' N; 3°37'E) at 2117 m water depth (Fig. 1). The sediment consists of brown nannofossil and foraminifera silty clay and includes pteropods rich-layers, gastropods fragments and dark layers. A light bioturbation is often visible (Cisneros et al., 2016).

2.2 - Coccoliths

Coccolith analysis was carried every 0.5-1 cm, for a total of 42 samples, which were analysed with a polarized microscope at ~ 1000× magnification. Rippled smear slides were prepared following standard procedures (Bown and Young, 1998) on the < 63 μm sediment residue. 1000 specimens were identified following the taxonomic concepts of Young et al., (2003) and Jordan et al. (2004). Taxa were grouped in 'placoliths', 'miscellaneous group', 'upper photic zone (UPZ) group', 'lower photic zone (LPZ) group' and 'holococcoliths' (Di Stefano and Incarbona, 2004; Incarbona et al., 2010). Placoliths include *Emiliania huxleyi*, small *Gephyrocapsa*, *Gephyrocapsa muellerae*, and *Gephyrocapsa oceanica*. The miscellaneous group includes *Helicosphaera* spp., *Coccolithus pelagicus*, *Syracosphaera histrica*, *Pontosphaera* spp., *Calcidiscus leptoporus*, *Coronosphaera* spp., *Braarudosphaera bigelowii*, *Oolithotus fragilis*, *Syracosphaera pulchra*, *Umbilicosphaera sibogae*, *Ceratolithus* spp., *Calciosolenia* spp., and specimens of all the other species. UPZ group includes *Umbellosphaera* spp., *Rhabdosphaera* spp. and *Discosphaera tubifera*. LPZ group includes *F. profound* and a negligible number of *Gladiolithus flabellatus* specimens. Holococcoliths

include all the coccoliths produced during the haploid life-cycle stage (Incarbona, et al., 2019a).

The N ratio is used to reconstruct the nutricline dynamics and is calculated following Flores et al. (2000): small placoliths / (small placoliths + *F. profunda*), where small placoliths are *E. huxleyi*, small *Gephyrocapsa* and *G. muellerae*. High values in the N ratio indicate a shallow nutricline, while low values in the N ratio indicate a deep nutricline.

The Shannon-Wiener diversity H-index was assessed by:

$H = -\sum[(p_i) * \log(p_i)]$

where $p_i = n/N$

and where n is the number of coccoliths of a given species and N is the total number of coccoliths of the assemblage.

2.3 - Chronology

The MR3.3 core chronology follows Cisneros et al. (2016). Summarizing, the age model was assessed by 6 AMS $\Delta^{14}C$ dates and two eco-bio-stratigraphic horizons in a Bayesian deposition model by the Bacon software with the statistical package R. A tuning between Mg/Ca SST variations and Mn peaks was carried out with the companion HER-MC-MR3.1 and 3.2 cores, where ^{210}Pb and ^{137}Cs activity profiles were also acquired. Any readjustment from the tuning was within the 95% confidence level of the Bayesian age model. The average sedimentation rate is 11.0 cm/kyr, the average coccolith analysis resolution is 62 years from the base of the core up to sample 15-16 cm (where the sampling pace was every 1 cm) and 36 years from sample 14.5-15 cm to the top of the core (where the sampling pace was every 0.5 cm).

2.4 – Spectral analysis

The analysis of non-stationary (frequency changes with time) and non-linear signals was performed by applying the Ensemble Empirical Mode Decomposition algorithm (EEMD) by Wu and Huang (2009).

The EEMD is adaptive noise-assisted data analysis method, that improves the ordinary Empirical Mode Decomposition (EMD) by Huang et al. (1998). This decomposition provides a powerful method to investigate the different processes behind a given time series data and separates short time-scale events from a general trend. This technique relies upon the assumption that any complicated signal can be decomposed into a finite and often small number of components called “Intrinsic Mode Functions” (IMFs) (Huang et al., 1998). Each IMF represents an embedded characteristic simple oscillation on a separated timescale. The

IMF components were analysed with "REDFIT" and Cross-wavelet transform (XWT). All data were detrended prior to analysis. All analyses were carried out with R (version 4.1.3) using Rlibeemd (Luukko et al.2016), dplR (Bunn, 2010), and WaveletComp (Roesch and Schmidbauer, 2014) packages.

3 - Coccolithophore ecology and surveys

Placoliths are 'r-strategist' taxa, rapidly exploit nutrients in the photic zone, (Young, 1994). In the Mediterranean Sea, placoliths bloom in winter, after nutrient fertilization from deeper water layers, when the water column is mixed (Di Stefano et al., 2011; Keuter et al., 2022; Knappertsbusch, 1993; Triantaphyllou et al., 2004; Ziveri et al., 2000; Rutten et al., 2000). *Florisphaera profunda* is a deep photic zone species, whose high relative abundance is linked to the occurrence of a deep nutricline (McIntyre and Molfino, 1996; Molfino and McIntyre, 1990). In low- and middle-latitude open ocean regions, the abundance of *F. profunda* is a proxy for primary productivity (Beaufort et al., 2001, 1997; Hernández-Almeida et al., 2019). In the Mediterranean Sea, except for a limited area in the central part of the basin, there is no apparent relationship between *F. profunda* abundance and satellite-observed primary productivity values (Hernández-Almeida et al., 2019; Incarbona et al., 2008). However, *F. profunda* has been generally used to decipher water column stratification and development of a deep nutricline due to monsoon-fueled freshwater discharge in the eastern Mediterranean (Castradori, 1993; Grelaud et al., 2012; Incarbona et al., 2019a; Incarbona et al., 2022; Negri et al., 1999; Triantaphyllou et al., 2009b).

UPZ are so-called 'K-strategist' taxa. They are specialized to exploit a minimum uptake of nutrients in surface water when a deep summer thermochline takes place (Bazzicalupo et al., 2020; Di Stefano and Incarbona, 2004; Incarbona et al., 2013; Young, 1994). Miscellaneous taxa reflect the lack of distinctive ecological preference, with a possible weak K-strategy (Incarbona et al., 2010b; Young, 1994). Holococcoliths prefer dwelling in warm, oligotrophic surface water, like UPZ taxa (D'Amario et al., 2017; Kleijne, 1991; Knappertsbusch, 1993; Oviedo et al., 2015). Preservation of holococcoliths improves when dense water renewal ensures vigorous ventilation/oxygenation of the seafloor and gets worse in sapropel layers (Crudeli et al., 2006; Incarbona et al., 2019a; Incarbona et al., 2022; Incarbona and Di Stefano, 2019).

4 – Study Area

The Mediterranean anti-estuarine circulation pattern is forced by its negative hydrological balance (Robinson and Golnaraghi, 1994). Surface water enters the Gibraltar Strait (Modified Atlantic Water - MAW) and occupies the first 100-200 m of the water column. MAW flows along the North African coast and reaches the Sicily Strait (Millot, 1999), where it is split (Robinson et al., 1999) into the Tyrrhenian Sea, along the northern coast of Sicily and the Italian Peninsula (Millot, 1999) (Fig. 1). The flows of MAW west and east of Corsica join and form the Liguro-Provenço-Catalan Current, also called Northern Current, which is extended at least as far as the Channel of Ibiza (Millot, 1999). An intense thermal front is found between the Gulf of Lions, where relatively cool Northwesterlies blow, and the Balearic Sea that is far less windy (Millot, 1999). Part of the Liguro-Provenço-Catalan Current continues southward from the Channel of Ibiza, but with less energy and tends to enter the Alboran Sea where it encounters the energetic flow of recent MAW (Millot, 1999) (Fig. 1).

Levantine Intermediate Water (LIW) formation occurs in the eastern Mediterranean in winter, due to surface cooling on salt-enriched water masses (Malanotte-Rizzoli et al., 2014; Malanotte-Rizzoli and Hecht, 1988) and is established at 200-600 m depth. LIW crosses the Sicily Channel and flows into the Tyrrhenian Sea (Lermusiaux and Robinson, 2001; Millot, 1999). LIW maintains almost unaltered values of temperature and salinity (14.0-14.5 °C and about 38.5 ‰) from the Ligurian Sea and the Gulf of Lions to the Balearic and Alboran Seas (Millot, 1999) and is the main source of Mediterranean Outflow Water which passes through the Gibraltar Strait. Deep water formation takes place in the Gulf of Lions (Western Mediterranean Deep Water - WMDW) and in the Adriatic and Aegean Seas (Eastern Mediterranean Deep Water), where permanent cyclonic gyres are established. In the Gulf of Lions, Mistral winds produce surface water cooling and evaporation in winter, leading to water column convection, mixing up with LIW and sinking to the seafloor (Malanotte-Rizzoli et al., 2014; Pinardi and Masetti, 2000; Rohling et al., 2015). Dense shelf water cascading in winter and early spring is a further mechanism that may contribute to the sink of water to the seafloor (Canals et al., 2006). WMDW production from convection is thought to be the most relevant process for deep water renewal and may occur while dense shelf water cascading is weak (Durrieu de Madron et al., 2017).

The transition between the subtropical high-pressure belt over North Africa and westerlies over central and western Europe control seasonal atmospheric variations in the Mediterranean/European region. The displacement of this transition leads to high-pressure established in summer and penetration of northern storm tracks in winter (Rohling et al., 2015). The Mediterranean region is mainly influenced by the North Atlantic Oscillation

(NAO). During positive NAO-index phases, westerlies blow over the western parts of northern Europe, while dry conditions are experienced in southern Europe and northern Africa and *vice versa* during negative NAO-index phases (Comas-Bru and McDermott, 2014). However, a very limited impact on modern WMDW production is observed by NAO variability, especially in comparison with the East Atlantic pattern, whose North-South pressure dipole is centred between Greenland and Scandinavia (Josey et al., 2011; Rutten et al., 2000).

5 – Results

Coccoliths in MR3.3 core are always abundant, well preserved and diversified. The distribution patterns of selected taxa are shown in Figures 2 and briefly commented below. *Emiliania huxleyi* < 4μm is the dominant species (71.9-80.2%, 75.6% on average) and shows a general increasing abundance trend to the top of the record (Fig. 2). *Emiliania huxleyi* > 4μm abundance is between 0.0 and 2.2% and increases during the LIA (Fig. 2). *Florisphaera profunda* is the second most abundant species, (7.0-13.8%, 11.3% on average), and shows several statistically significant variations, with minima centered on the end of the TP, on the end of the Dark Age, in part of MCA and on LIA (Fig. 2). Among gephyrocapsids, small *Gephyrocapsa* (1.8-8.8%) shows a decreasing abundance trend since the Dark Age, *G. oceanica* (0.0-0.9%) is always rare and its distribution pattern is rather scattered since the MCA (Fig. 2). Holoccoliths (0.1-2.3%, 1.1% on average) show several abrupt abundance fluctuations throughout the record, that despite the low magnitude are often significant at a 95 % confidence level (Fig. 2).

All the other coccolith taxa exhibit abundance values < 2% (Coccolith raw data are available in Supplementary Data Table 1). *Umbellosphaera* spp. and *Rhabdosphaera* spp. do not show significant abundance fluctuations. *Discosphaera tubifera* is absent during Dark Age and the early MCA. *Calcidiscus leptoporus*, *S. pulchra*, *S. histrica*, *Coronosphaera* spp., *Helicosphaera carteri*, *Helicosphaera pavimentum*, *U. sibogae* and *Calciosolenia* spp. are generally more abundant in the upper part of the record and during the cold TP, Dark Age and LIA.

The most significant result from grouping coccolith taxa is the continuous opposite pattern (both abundance fluctuations and trend) between placoliths and *F. profunda* (LPZ group) (Fig. 3), whose $R^2 = 0.66$ (Fig. 4). Significant R indices, evaluated by student T-tests ($p < 0.005$) among different coccolith groups are summarized in Table 1 and shown in Figure 4. Though six group relationships passed the student T-test (Tab. 1), scatter plots in Fig. 4 show the little significance for most of them, in terms of correlation Index (R^2) values. The miscellaneous

group exhibits at least one significant abundance fluctuation, centred around the Dark and a distinctive positive trend since the MCA (Fig. 3). This is an important result, given that abundance changes in individual species do not cross the treshold of 95% confidence level. Miscellaneous group and holococcoliths share the same abundance variation pattern (Fig. 3), but the $R^2 = 0.27$ is not significant. The UPZ group do not show any significant abundance fluctuation, even though its abundance since the latest MCA is on average higher than before (Fig. 5). The only correlation index value significant, except that already mentioned between placoliths and *F. profunda*, is the $R^2 = 0.42$ between the Miscellaneous group and *F. profunda* (Fig. 6), that show opposite patterns and fluctuations somewhere in the record (Fig. 5).
The Shannon Wiener index shows abrupt and repeated values changes between 2.0 and 3.2, with higher frequency modifications since the Dark ages (Fig. 2). High diversity peaks since the MCA are due to increased percentage abundances of *F. profunda* and miscellaneous group taxa (Figs. 2-3).

6 – Discussion

6.1 – Solar activity and nutricline depth variations

Placoliths and *F. profunda* are anticorrelated throughout the MR3.3 core record (Fig. 3-4) and their relative abundance fluctuations indicate nutricline depth variations within the photic zone (Bazzicalupo et al., 2018, 2020; Colmenero-Hidalgo et al., 2004; Di Stefano et al., 2015; Flores et al., 2000; Incarbona et al., 2008, 2013; Incarbona et al., 2010a, b; Incarbona et al., 2022). The shallow nutricline associated to a higher number of placolith and *vice versa* a deep nutricline for a higher number of *F. profunda* specimens is summarized by the N-ratio (Fig. 5A). The comparison with the Total Solar Irradiance (TSI) (Steinhilber et al., 2009) clearly address a tight relationship, with a deep nutricline associated with high TSI and a shallow nutricline associated to solar activity minima (Fig. 5B). The solar forcing may have acted directly on the water column dynamics, favoring the summer thermocline deepening during phases of high irradiance and thus establishing a deep photic zone stratification that fosters *F. profunda* cells proliferation (Hernández-Almeida et al., 2019; Incarbona et al., 2008; Incarbona et al., 2010b). The comparison with *G. ruber* $\delta^{18}O$ values in the MR3.3 core (Margaritelli et al., 2018), suggests the occurrence of warmer/fresher summer surface water (Rohling et al., 2004) associated with a deep nutricline over the studied record (Fig. 5C). The TSI forcing may also have acted indirectly on the Balearic Sea water column dynamics, promoting the occurrence of severe winter conditions in Europe and in the Mediterranean Sea during solar minima, by the long-lasting advection of cold air from the Arctic or blocking events in the

eastern Atlantic (Brugnara et al., 2013; Lockwood et al., 2010; Sirocko et al., 2012). Strong northerly wind events may in turn have caused the southward displacement of the North Balearic Front and the subsequent SST cooling and erosion of the water column stratification, as recently observed in oceanographic surveys and numerical modelling (Seyfried et al., 2019). The advection of northern cold air masses in the northwestern Mediterranean Sea and the southward displacement of the North Balearic Front associated with a shallow nutricline in the Balearic Sea during Roman, Oort, Wolf, Spörer and Maunder TSI minima is supported by lower foraminiferal Mg/Ca-derived SST in MR-3.3 core, that according to *G. bulloides* ecology in the Balearic Sea should primarily reflect spring SST (Cisneros et al., 2016; Rigual-Hernández et al., 2012), and cold episodes in the Mediterranean SST stack (Marriner et al., 2022) (Fig. 5D-E).

The solar activity fingerprint in the *F. profunda*'s MR-3.3 record is clearly visible by the power spectrum, with significant periodicities at 231, 317 and 613 years and by comparison with TSI in the IMF5 component (Fig. 6A-B). The 231 years periodicity (over the CI 99%) is referred to the well-known de Vries-Suess cycle and it has been already found in the *F. profunda* record of the central Mediterranean Sea over the whole Holocene and over the last four centuries (Incarbona et al., 2008; Incarbona et al., 2010b). The 317- and 613-years periodicity match with ~350-years and with 500-700 periodicities found in solar activity proxies over the Holocene in Antarctic ice cores (Soon et al., 2014). The cross-wavelet analysis between *F. profunda* percentage values and the TSI shows that the 500-700 years signal is present throughout the last 2700 years and that higher frequency signals emerge since the Dark Age (Fig. 6C). The match between *F. profunda* abundance changes in the Balearic Sea and TSI values provides further evidence that solar variability is a main climatic forcing for water column and phytoplankton dynamics during the preindustrial age.

A recent climate simulation suggested that, during insolation minima, an atmospheric pattern like the East Atlantic/Western Russian developed over the Mediterranean region, which favors continental cold winds to penetrate the Aegean Sea and blocks their influence in the Gulf of Lions (Cortina-Guerra et al., 2021). This atmospheric pattern, and the subsequent SST gradient between the two Mediterranean subbasins, would explain the slight delay of N-ratio peaks, with respect to Roman, Oort, Wolf, and Spörer TSI minima (Fig. 5A-B), that the cross-correlation analysis estimates in a 50-60-year lag (Fig. 6D).

Coccolithophore geographic distribution is mainly influenced by hydrology (surface and subsurface currents, fronts) and water column dynamics, rather than solely SST. However, *E. huxleyi* > 4μm specimens seem to be a tracer of cold surface water masses in the Atlantic

Ocean and Mediterranean Sea sediments of the latest Pleistocene (Colmenero-Hidalgo et al., 2004; Flores et al., 2010). The amount of large *E. huxleyi* specimens in the Mediterranean during the Holocene is largely negligible (Colmenero-Hidalgo et al., 2004; Di Stefano et al., 2015), as in the pre-industrial Balearic Sea, where values are < 2.5 % (Fig. 5F). Though the low abundance variability, *E. huxleyi* > 4μm shows a distinctive peak within the Dark Age (coinciding with the Roman TSI minimum) and values significantly above the average in the LIA (coinciding with Wolf, Spörer and Maunder TSI minima), suggesting its high sensitivity to slight SST changes, whose magnitude is < 2°C (Fig. 5).

Percentage values of the deep photic zone *F. profunda* in sediment cores are used for quantitative primary paleoproductivity reconstruction at low- and middle-latitude, after calibration by satellite-derived productivity estimates (Hernández-Almeida et al., 2019). In the Mediterranean Sea, the relationship between *F. profunda* relative abundance and primary productivity estimates is questioned (Hernández-Almeida et al., 2019). Living coccolithophore data from six and five stations in the area (around Balearic Islands and in the Gulf of Lions) were respectively recovered by the Vicomed I (September-October) and II (February-March) expeditions (white and yellow stars in Fig. 1) (Knappertsbusch, 1993). A relevant amount of *F. profunda* cells is found just in two stations during the summer-autumn cruise, and unexpectedly, in a station in winter (Knappertsbusch, 1993). A consistent distribution of *F. profunda* cells compared to hydrological parameters (e.g. SST, thermocline depth) is not evident for both Vicomed I and II. Maybe, this is due to the too short interval of the investigation that obscure coccolithophore blooming episodes, detected by long-series investigation, such as trap sediments (Auliaherliaty et al., 2009; Hernández-Almeida et al., 2011; Ziveri et al., 2000). However, at least the linear trend of nutricline shallowing before the Second Industrial Revolution (~ 1850 CE) is consistent with the same trend in planktonic foraminifera proxies for surface water productivity (Fig. 5G) and deep chlorophyll maximum (Fig. 5H) (Margaritelli et al., 2018). Thus, coccolith and planktonic foraminiferal data in core MR-3.3 would respectively confirm a sustained nutricline shallowing and productivity increase in the pre-industrial central-western Mediterranean (Incarbona et al., 2010b, 2019b; Margaritelli et al., 2018; Pallacks et al., 2021).

6.2 – Holococcolith preservation and deep-water production

Holococcoliths (coccoliths produced by different species during the haploid phase of the life cycle) behave as unique ecological category, with a distinct preference for warm and oligotrophic surface waters (D'Amario et al., 2017). In the Mediterranean

sedimentary record, holococcolith abundance is tightly controlled by preservation, which is enhanced by seafloor ventilation (Crudeli et al., 2006; Di Stefano et al., 2015; Incarbona et al., 2019a; Incarbona and di Stefano, 2019). In core MR-3.3, most of the holococcoliths belong to the species *Calyptrosphaera oblonga*, as for Holocene sapropel S1 studies (Crudeli et al., 2006; Di Stefano et al., 2015; Incarbona et al., 2019a; Incarbona et al., 2022; Incarbona and Di Stefano, 2019), suggesting the prevalent action of seafloor selective preservation in shaping their distribution. Thus, holococcoliths would indicate different episodes of increased seafloor ventilation during the end of TP and of Dark Age, and across part of the MCA and of LIA, rather than changes in paleoecological conditions (Fig. 7A).

The recent (last few millennia) history of the Mediterranean deep-water formation, either in the western or eastern Mediterranean Sea, is still unclear. Organic geochemical proxies point to enhanced Aegean Sea deep-water formation during MCA and the earliest LIA (Fig. 7B) (Gogou et al., 2016), possibly linked to recurrent Eastern Mediterranean Transient-like episodes, during which water exchange in the Sicily Channel was enhanced (Incarbona et al., 2016). In the western Mediterranean, the non-cohesive silt fraction (UP10) records, whose oscillations follow the deep-water circulation strength, have been recently acquired for the here studied location (Fig. 7C) (Cisneros et al., 2019).

In the studied record, holococcolith enhanced preservation is in line with $\delta^{18}O$ negative values of the Cueva de Asiul speleothem (Fig. 7D), which marks increased rainfall in North Spain (Smith et al., 2016). In their original work, Smith et al. (2016) interpreted $\delta^{18}O$ negative values as a result of Atlantic wet air masses advection into the western Mediterranean, like today's NAO negative phases. However, the $\delta^{18}O$ Cueva de Asiul speleothem variability seems to be different from current NAO reconstructions (Faust et al., 2016; Olsen et al., 2012; Trouet, 2009), for instance during the MCA (Fig. 7F). In any case, independently from the NAO pattern, it is evident that enhanced holococcolith preservation match with increased North Spain rainfall during the middle MCA and LIA and even during TP and Dark Ages (Fig. 7). A closer speleothem record from Mallorca Island (Fig. 7E) (Cisneros et al., 2021) provides further evidence that holococcolith enhanced preservation occurred when speleothem $\delta^{18}O$ negative values suggest enhanced rainfall in this part of the Mediterranean Sea. In this speleothem composite record, a hiatus exists for the MCA and early LIA, but the late LIA wet phase (~ 1700 CE), coincides with the last holococcolith abundance peak (Fig. 7).

Increased North Spain and Mallorca rainfall implies the advection of strong and prolonged westerlies, possibly by long-lasting blocking events that modifies their blow and thus impacting western Europe (Margaritelli et al., 2020). Blockings and prolonged westerlies

action may be among the main triggers for deep-water formation (Cacho et al., 2000; Moreno et al., 2005), promoting seafloor ventilation and holococcolith preservation. Abundance peaks of planktonic foraminifera *Globorotalia truncatulinoides* during MCA and LIA suggest the occurrence of a winter deep mixed layer in the Balearic Sea (Margaritelli et al., 2018; 2020) and support the strengthened atmospheric circulation.

Holococcolith preservation is also in good match with the lightest *G. bulloides* $\delta^{18}O$ seawater values in the same MR-3.3 core (Fig. 7G). There at least two possible explanations for this relationship, linked to prolonged wind action, enhanced deepwater formation in the Gulf of Lions and the southward shift of the North Balearic Front: 1) the arrival in the Minorca Rise area of Rhone River freshwater plumes (Barral et al., 2021), that would be in agreement with enhanced rainfall from Spain speleothems (Figs. 7D-E); 2) the arrival of meso-scale eddies associated to the Algerian Current, characterized by lower salinity from not or little modified (poorly vertically mixed) Atlantic surface water (Barral et al., 2021).

The holococcolith distribution pattern is instead apparently quite different from the UP10 record from Nmin1 and Nmin2 cores (Fig. 7C) (Cisneros et al., 2019). The UP10 data were interpreted as a proxy for deep convection in the Gulf of Lions, and thus they provide an apparently conflicting view with the here presented results. However, looking at numerical sills in the UP10 records that would determine deepwater formation events (> 37.5% in Nmin1 and > 42.5% in Nmin2 cores, see red and blue fillings in Fig. 7C curves), the strongest discrepancy may be restricted to the RP. Nevertheless, the holococcoliths and UP10 proxies have a very different nature and thus respond to different environmental variables related to WMDW formation in the Gulf of Lions. On one side, holococcoliths should be rather tied to seafloor ventilation conditions (oxygen content and seawater carbonate chemistry, see Incarbona et al., 2019a; Incarbona et al., 2022) while UP10 should reflect bottom current strength (physical features like speed, see Cisneros et al., 2019). Such chemical and physical variables could not always have an equal response in front to different WMDW formation mechanisms (i.e. preferentially record deep water convection *versus* dense shelf water cascading). In any case, the combination of the two micropaleontological and sedimentological proxies suggests the intermittent operation of the Gulf of Lions over the pre-industrial period which needs to be further explored with a wider range of proxies and records.

7 – Conclusion

In the Balearic Sea, northwestern Mediterranean Sea, significant abundance variations in coccolith assemblages were associated with historical/cultural periods: Talaiotic period, base

of the record – 0 CE; Roman warm period, 0-400 CE; Dark Age, 400-800 CE; Medieval Climate Anomaly, 800-1250 CE; Little Ice Age, 1250-1850 CE (Büntgen et al., 2016; Neukom et al., 2019).

We found that the *F. profunda*-derived nutricline depth was modified by TSI forcing. A shallow nutricline was established in the water column while solar activity is at minima. The TSI forcing may have promoted severe winters in Europe and in the Mediterranean Sea during solar minima, by the long-lasting advection of cold air from the Arctic or blocking events in the eastern Atlantic. Strong northerly wind events may in turn have caused the southward displacement of the North Balearic Front and the subsequent SST cooling and erosion of the water column stratification. The spectral analysis on *F. profunda* abundance showed significant periodicities at 231, 317 and 613 years, all of them found in solar activity proxies over the Holocene in Antarctica ice cores, including the de Vries-Suess cycle. These results provide evidence that solar variability is a main climatic forcing for water column and phytoplankton dynamics during the preindustrial age in the Mediterranean Sea.

Holococcolith enhanced preservation was in line with $\delta^{18}O$ negative values of the Cueva de Asiul and Mallorca speleothems, which mark increased rainfall in the western Mediterranean region. Increased rainfall would have implied the advection of strong and prolonged westerlies, possibly by long-lasting blocking events that modifies their blow and thus impacting western Europe and would have triggered deep-water formation and seafloor ventilation. The holococcolith distribution pattern is instead apparently quite different from the UP10 record, especially for the RP, probably as a result of the different nature of the proxies that make them sensitive to chemical and physical changes respectively. In any case, both proxy records suggest the intermittent activity of deep-water formation in the Gulf of Lions over the pre-industrial period.

Acknowledgments

The cores HER-MC-MR3.1A/3.3 has been collected aboard of R/V Hespérides. AI acknowledges the support received from the NBFC, funded by the Italian Ministry of University and Research, PNRR, Missione 4 Componente 2, 'Dalla ricerca all'impresa', Investimento 1.4, project CN00000033. This research has been financially supported by ERC-Consolidator TIMED project (REP-683237). This research is contributing to the BIOCAL project (PID2020-113526RB).

Bibliographic references

Auliaherliaty, L., Stoll, H.M., Ziveri, P., Malinverno, E., Triantaphyllou, M.V., Stravrakakis, S., Lykousis, V., 2009. Coccolith Sr/Ca ratios in the eastern Mediterranean: Production versus export processes. Mar Micropaleontol 73, 196–206. https://doi.org/10.1016/j.marmicro.2009.10.001

Ausín, B., Flores, J.A., Sierro, F.J., Bárcena, M.A., Hernández-Almeida, I., Francés, G., Gutiérrez-Arnillas, E., Martrat, B., Grimalt, J.O., Cacho, I., 2015. Coccolithophore productivity and surface water dynamics in the Alboran Sea during the last 25kyr. Palaeogeogr Palaeoclimatol Palaeoecol 418, 126–140. https://doi.org/10.1016/j.palaeo.2014.11.011

Balestrieri, C., Ziveri, P., Grelaud, M., Mortyn, P.G., Agnini, C., 2021. Enhanced E. huxleyi carbonate counterpump as a positive feedback to increase deglacial pCO2sw in the Eastern Equatorial Pacific. Quat Sci Rev 260, 106921. https://doi.org/https://doi.org/10.1016/j.quascirev.2021.106921

Barral, Q.-B., Zakardjian, B., Dumas, F., Garreau, P., Testor, P., Beuvier, J., 2021. Characterization of fronts in the Western Mediterranean with a special focus on the North Balearic Front. Prog Oceanogr 197, 102636. https://doi.org/https://doi.org/10.1016/j.pocean.2021.102636

Baumann, K.-H., Andruleit, H., Böckel, B., Geisen, M., Kinkel, H., 2005. The significance of extant coccolithophores as indicators of ocean water masses, surface water temperature, and paleoproductivity: a review. Paläontol Z 79, 93–112. https://doi.org/10.1007/bf03021756

Bazzicalupo, P., Maiorano, P., Girone, A., Marino, M., Combourieu-Nebout, N., Incarbona, A., 2018. High-frequency climate fluctuations over the last deglaciation in the Alboran Sea, Western Mediterranean: Evidence from calcareous plankton assemblages. Palaeogeogr Palaeoclimatol Palaeoecol. https://doi.org/10.1016/j.palaeo.2018.06.042

Bazzicalupo, P., Maiorano, P., Girone, A., Marino, M., Combourieu-Nebout, N., Pelosi, N., Salgueiro, E., Incarbona, A., 2020. Holocene climate variability of the Western Mediterranean: Surface water dynamics inferred from calcareous plankton assemblages. Holocene 30. https://doi.org/10.1177/0959683619895580

Beaufort, L., de Garidel-Thoron, T., Mix, A.C., Pisias, N.G., 2001. ENSO-like forcing on oceanic primary production during the Late Pleistocene. Science 293, 2440–2444. https://doi.org/10.1126/science.293.5539.2440

Beaufort, L., Lancelot, Y., Camberlin, P., Cayre, O., Vincent, E., Bassinot, F., Labeyrie, L., 1997. Insolation Cycles as a Major Control of Equatorial Indian Ocean Primary Production. Science 278, 1451–1454.

Bonomo, S., Cascella, A., Alberico, I., Sorgato, S., Pelosi, N., Ferraro, L., Lirer, F., Vallefuoco, M., Bellucci, L., Agnini, C., Pappone, G., 2016. Reworked Coccoliths as runoff proxy for the last 400 years: The case of Gaeta Gulf (central Tyrrhenian Sea, Central Italy). Palaeogeogr Palaeoclimatol Palaeoecol 459, 15–28. https://doi.org/10.1016/j.palaeo.2016.06.037

Bown, Paul R., Young, J.R., 1998. Techniques, in: Bown, P.R. (Ed.), Calcareous Nannofossil Biostratigraphy. Chapman and Kluwer Academic, London, pp. 16–28.

Brugnara, Y., Brönnimann, S., Luterbacher, J., Rozanov, E., 2013. Influence of the sunspot cycle on the Northern Hemisphere wintertime circulation from long upper-air data sets. Atmos Chem Phys 13, 6275–6288. https://doi.org/10.5194/acp-13-6275-2013

Bunn A.G., 2010. Statistical and visual crossdating in R using the dplR library. Dendrochronologia, 28(4), 251–258. ISSN 1125-7865, doi:10.1016/j.dendro.2009.12.001

Büntgen, U., Myglan, V.S., Ljungqvist, F.C., McCormick, M., di Cosmo, N., Sigl, M., Jungclaus, J., Wagner, S., Krusic, P.J., Esper, J., Kaplan, J.O., de Vaan, M.A.C., Luterbacher, J., Wacker, L., Tegel, W., Kirdyanov, A. v, 2016. Cooling and societal change during the Late Antique Little Ice Age from 536 to around 660 AD. Nat Geosci 9, 231–236. https://doi.org/10.1038/ngeo2652

Cacho, I., Grimalt, J.O., Sierro, F.J., Shackleton, N., Canals, M., 2000. Evidence for enhanced Mediterranean thermohaline circulation during rapid climatic coolings. Earth Planet Sci Lett 183, 417–429. https://doi.org/10.1016/S0012-821X(00)00296-X

Canals, M., Puig, P., de Madron, X.D., Heussner, S., Palanques, A., Fabres, J., 2006. Flushing submarine canyons. Nature 444, 354–357. https://doi.org/10.1038/nature05271

Cascella, A., Bonomo, S., Salali, B., Sicre, M.-A., Pelosi, N., Schmidt, S., Lirer, F., 2019. Climate variability of the last ~2700 years in the Southern Adriatic Sea: Coccolithophore evidences. Holocene 30, 53–64. https://doi.org/10.1177/0959683619865600

Cascella, A., Bonomo, S., Lirer, F., Margaritelli, G., Checa, H., Cacho, I., Pena, L.D., Frigola, J., 2021. The response of calcareous plankton to the Sapropel S1 interval in North Ionian Sea. Glob Planet Change 205, 103599. https://doi.org/https://doi.org/10.1016/j.gloplacha.2021.103599

Castradori, D., 1993. Calcareous nannofossils and the origin of Eastern Mediterranean sapropel. Paleoceanography 8, 459–471.

Cisneros, M., Cacho, I., Frigola, J., Canals, M., Masqué, P., Martrat, B., Casado, M., Grimalt, J.O., Pena, L.D., Margaritelli, G., Lirer, F., 2016. Sea surface temperature variability in the

central-western Mediterranean Sea during the last 2700 years: A multi-proxy and multi-record approach. Climate of the Past 12, 849–869. https://doi.org/10.5194/cp-12-849-2016

Cisneros, M., Cacho, I., Frigola, J., Sanchez-Vidal, A., Calafat, A., Pedrosa-Pàmies, R., Rumín-Caparrós, A., Canals, M., 2019. Deep-water formation variability in the north-western Mediterranean Sea during the last 2500 yr: A proxy validation with present-day data. Glob Planet Change 177, 56–68. https://doi.org/https://doi.org/10.1016/j.gloplacha.2019.03.012

Cisneros, M., Cacho, I., Moreno, A., Stoll, H., Torner, J., Català, A., Edwards, R.L., Cheng, H., Fornós, J.J., 2021. Hydroclimate variability during the last 2700 years based on stalagmite multi-proxy records in the central-western Mediterranean. Quat Sci Rev 269, 107137. https://doi.org/https://doi.org/10.1016/j.quascirev.2021.107137

Colmenero-Hidalgo, E., Flores, J.A., Sierro, F.J., Bárcena, M.Á., Löwemark, L., Schönfeld, J., Grimalt, J.O., 2004b. Ocean surface water response to short-term climate changes revealed by coccolithophores from the Gulf of Cadiz (NE Atlantic) and Alboran Sea (W Mediterranean). Palaeogeogr Palaeoclimatol Palaeoecol 205, 317–336. https://doi.org/10.1016/j.palaeo.2003.12.014

Comas-Bru, L., McDermott, F., 2014. Impacts of the EA and SCA patterns on the European twentieth century NAO–winter climate relationship. Quarterly Journal of the Royal Meteorological Society 140, 354–363. https://doi.org/10.1002/qj.2158

Cortina-Guerra, A., Gomez-Navarro, J.J., Martrat, B., Montávez, J.P., Incarbona, A., Grimalt, J.O., Sicre, M.-A., Mortyn, P.G., 2021. Northern Hemisphere atmospheric pattern enhancing Eastern Mediterranean Transient-type events during the past 1000 years. Climate of the Past 17, 1523–1532. https://doi.org/10.5194/cp-17-1523-2021

Crudeli, D., Young, J.R., Erba, E., Geisen, M., Ziveri, P., de Lange, G.J., Slomp, C.P., 2006. Fossil record of holococcoliths and selected hetero-holococcolith associations from the Mediterranean (Holocene-late Pleistocene): Evaluation of carbonate diagenesis and palaeoecological-palaeocenographic implications. Palaeogeogr Palaeoclimatol Palaeoecol 237, 191–212. https://doi.org/10.1016/j.palaeo.2005.11.022

D'Amario, B., Ziveri, P., Grelaud, M., Oviedo, A., Kralj, M., 2017. Coccolithophore haploid and diploid distribution patterns in the Mediterranean Sea: Can a haplo-diploid life cycle be advantageous under climate change? J Plankton Res 39, 781–794. https://doi.org/10.1093/plankt/fbx044

Di Stefano, A., Foresi, L.M., Incarbona, A., Sprovieri, M., Vallefuoco, M., Iorio, M., Pelosi, N., di Stefano, E., Sangiorgi, P., Budillon, F., 2015. Mediterranean coccolith

ecobiostratigraphy since the penultimate Glacial (the last 145,000years) and ecobioevent traceability. Mar Micropaleontol 115. https://doi.org/10.1016/j.marmicro.2014.12.002

Di Stefano, E., Incarbona, A., 2004. High-resolution palaeoenvironmental reconstruction of ODP Hole 963D (Sicily Channel) during the last deglaciation based on calcareous nannofossils. Mar Micropaleontol 52. https://doi.org/10.1016/j.marmicro.2004.04.009

Di Stefano, E., Incarbona, A., Bonomo, S., Pelosi, N., 2011. Coccolithophores in water samples and fossil assemblages in sedimentary archives of the Mediterranean Sea: A review, in: Martorino, L., Puopolo, K. (Eds.), New Oceanography Research Developments: Marine Chemistry, Ocean Floor Analyses and Marine Phytoplankton. Nova Science Publishers, Inc., pp. 127–162.

Dittert, N., Baumann, K.H., Bickert, T., Henrich, R., Huber, R., Kinkel, H., Meggers, H., 1999. Carbonate dissolution in the Deep-Sea: Methods, Quantification and Paleoceanographic Application, in: Fischer, G., Wefer, G. (Eds.), Use of Proxies in Paleoceanography: Examples from the South Atlantic. pp. 255–284.

Drake, B.L., 2012. The influence of climatic change on the Late Bronze Age Collapse and the Greek Dark Ages. J Archaeol Sci 39, 1862–1870. https://doi.org/https://doi.org/10.1016/j.jas.2012.01.029

Durrieu de Madron, X., Ramondenc, S., Berline, L., Houpert, L., Bosse, A., Martini, S., Guidi, L., Conan, P., Curtil, C., Delsaut, N., Kunesch, S., Ghiglione, J.F., Marsaleix, P., Pujo-Pay, M., Séverin, T., Testor, P., Tamburini, C., collaboration, the A., 2017. Deep sediment resuspension and thick nepheloid layer generation by open-ocean convection. J Geophys Res Oceans 122, 2291–2318. https://doi.org/https://doi.org/10.1002/2016JC012062

Faust, J.C., Fabian, K., Milzer, G., Giraudeau, J., Knies, J., 2016. Norwegian fjord sediments reveal NAO related winter temperature and precipitation changes of the past 2800 years. Earth Planet Sci Lett 435, 84–93. https://doi.org/https://doi.org/10.1016/j.epsl.2015.12.003

Flores, J. A., Bárcena, M.A., Sierro, F.J., 2000. Ocean-surface and wind dynamics in the Atlantic Ocean off Northwest Africa during the last 140 000 years. Palaeogeogr Palaeoclimatol Palaeoecol 161, 459–478. https://doi.org/10.1016/S0031-0182(00)00099-7

Flores, J.A., Colmenero-Hidalgo, E., Mejía-Molina, A.E., Baumann, K.H., Henderiks, J., Larsson, K., Prabhu, C.N., Sierro, F.J., Rodrigues, T., 2010. Distribution of large Emiliania huxleyi in the Central and Northeast Atlantic as a tracer of surface ocean dynamics during the last 25,000years. Mar Micropaleontol 76, 53–66. https://doi.org/10.1016/j.marmicro.2010.05.001

Flores, J.A., Sierro, F.J., Francés, G., Vazquez, A., Zamarreno, I., 1997. The last 100,000 years in the western Mediterranean: sea surface water and frontal dynamics as revealed by coccolithophores. Mar Micropaleontol 29, 351–366.

Gogou, A., Triantaphyllou, M., Xoplaki, E., Izdebski, A., Parinos, C., Dimiza, M., Bouloubassi, I., Luterbacher, J., Kouli, K., Martrat, B., Toreti, A., Fleitmann, D., Rousakis, G., Kaberi, H., Athanasiou, M., Lykousis, V., 2016. Climate variability and socio-environmental changes in the northern Aegean (NE Mediterranean) during the last 1500 years. Quat Sci Rev 136, 209–228. https://doi.org/10.1016/j.quascirev.2016.01.009

Grelaud, M., Marino, G., Ziveri, P., Rohling, E.J., 2012. Abrupt shoaling of the nutricline in response to massive freshwater flooding at the onset of the last interglacial sapropel event. Paleoceanography 27. https://doi.org/10.1029/2012PA002288

Hernández-Almeida, I., Ausín, B., Saavedra-Pellitero, M., Baumann, K.-H., Stoll, H.M., 2019. Quantitative reconstruction of primary productivity in low latitudes during the last glacial maximum and the mid-to-late Holocene from a global Florisphaera profunda calibration dataset. Quat Sci Rev 205, 166–181. https://doi.org/https://doi.org/10.1016/j.quascirev.2018.12.016

Hernández-Almeida, I., Bárcena, M.A., Flores, J.A., Sierro, F.J., Sanchez-Vidal, A., Calafat, A., 2011. Microplankton response to environmental conditions in the Alboran Sea (Western Mediterranean): One year sediment trap record. Mar Micropaleontol 78, 14–24. https://doi.org/10.1016/j.marmicro.2010.09.005

Hodell, D. a, Brenner, M., Curtis, J.H., Guilderson, T., 2001. Solar forcing of drought frequency in the Maya lowlands. Science 292, 1367–1370. https://doi.org/10.1126/science.1057759

Huang N.E., Shen Z., Long S.R., Wu M.C., Shih H.H., Zheng Q., Yen N.C., Tung C.C., Liu H.H., 1998. The empirical mode decomposition and the Hilbert spectrum for nonlinear and non-stationary time series analysis. Proc. R. Soc. Lond. A. Math., 454, 903–995.

Incarbona, A., Abu-Zied, R.H., Rohling, E.J., Ziveri, P., 2019a. Reventilation Episodes During the Sapropel S1 Deposition in the Eastern Mediterranean Based on Holococcolith Preservation. Paleoceanogr Paleoclimatol 34, 1597–1609. https://doi.org/10.1029/2019PA003626

Incarbona, A., Di Stefano, E., 2019. Calcareous nannofossil palaeoenvironmental reconstruction and preservation in sapropel S1 at the Eratosthenes Seamount (Eastern Mediterranean). Deep Sea Res 2 Top Stud Oceanogr 164. https://doi.org/10.1016/j.dsr2.2018.10.004

Incarbona, A, di Stefano, E., Patti, B., Pelosi, N., Bonomo, S., Mazzola, S., Sprovieri, R., Tranchida, G., Zgozi, S., Bonanno, A., 2008. Holocene millennial-scale productivity variations in the Sicily Channel (Mediterranean Sea). Paleoceanography 23, 1–18. https://doi.org/10.1029/2007PA001581

Incarbona, A., Jonkers, L., Ferraro, S., Sprovieri, R., Tranchida, G., 2019b. Sea Surface Temperatures and Paleoenvironmental Variability in the Central Mediterranean During Historical Times Reconstructed Using Planktonic Foraminifera. Paleoceanogr Paleoclimatol 34, 394–408. https://doi.org/10.1029/2018PA003529

Incarbona, A., Marino, G., di Stefano, E., Grelaud, M., Pelosi, N., Rodríguez-Sanz, L., Rohling, E.J., 2022. Middle-Late Pleistocene Eastern Mediterranean nutricline depth and coccolith preservation linked to Monsoon activity and Atlantic Meridional Overturning Circulation. Glob Planet Change 103946. https://doi.org/https://doi.org/10.1016/j.gloplacha.2022.103946

Incarbona, A., Martrat, B., Di Stefano, E., Grimalt, J.O., Pelosi, N., Patti, B., Tranchida, G., 2010a. Primary productivity variability on the Atlantic Iberian Margin over the last 70,000 years: Evidence from coccolithophores and fossil organic compounds. Paleoceanography 25. https://doi.org/10.1029/2008PA001709

Incarbona, A., Martrat, B., Mortyn, P.G., Sprovieri, M., Ziveri, P., Gogou, A., Jordà, G., Xoplaki, E., Luterbacher, J., Langone, L., Marino, G., Rodríguez-Sanz, L., Triantaphyllou, M., Di Stefano, E., Grimalt, J.O., Tranchida, G., Sprovieri, R., Mazzola, S., 2016. Mediterranean circulation perturbations over the last five centuries: Relevance to past Eastern Mediterranean Transient-type events. Sci Rep 6. https://doi.org/10.1038/srep29623

Incarbona, A., Sprovieri, M., di Stefano, A., Di Stefano, E., Salvagio Manta, D., Pelosi, N., Ribera d'Alcalà, M., Sprovieri, R., Ziveri, P., 2013. Productivity modes in the mediterranean sea during dansgaard-oeschger (20,000-70,000yr ago) oscillations. Palaeogeogr Palaeoclimatol Palaeoecol 392. https://doi.org/10.1016/j.palaeo.2013.09.023

Incarbona, A., Ziveri, P., Di Stefano, E., Lirer, F., Mortyn, G., Patti, B., Pelosi, N., Sprovieri, M., Tranchida, G., Vallefuoco, M., Albertazzi, S., Bellucci, L.G., Bonanno, A., Bonomo, S., Censi, P., Ferraro, L., Giuliani, S., Mazzola, S., Sprovieri, R., 2010b. The Impact of the Little Ice Age on Coccolithophores in the Central Mediterranea Sea. Climate of the Past 6, 795–805. https://doi.org/10.5194/cp-6-795-2010

Jordan, R.W., Cros, L., Young, J.R., 2004. A revised classification scheme for living haptophytes. Micropaleontology 50, 55–79. https://doi.org/10.2113/50.Suppl_1.55

Josey, S.A., Somot, S., Tsimplis, M., 2011. Impacts of atmospheric modes of variability on Mediterranean Sea surface heat exchange. J Geophys Res Oceans 116, 1–15. https://doi.org/10.1029/2010JC006685

Keuter, S., Silverman, J., Krom, M.D., Sisma-Ventura, G., Yu, J., Tsemel, A., Ben-Ezra, T., Sher, D., Reich, T., Koplovitz, G., Frada, M.J., 2022. Seasonal patterns of coccolithophores in the ultra-oligotrophic South-East Levantine Basin, Eastern Mediterranean Sea. Mar Micropaleontol 175, 102153. https://doi.org/https://doi.org/10.1016/j.marmicro.2022.102153

Kleijne, A., 1991. Holococcolithophorids from the Indian-Ocean, Red-Sea, Mediterranean-Sea and North-Atlantic Ocean. Mar Micropaleontol 17, 1–76. https://doi.org/Doi 10.1016/0377-8398(91)90023-Y

Knappertsbusch, M., 1993. Geographic distribution of living and Holocene coccolithophores in the Mediterranean Sea. Mar Micropaleontol. https://doi.org/10.1016/0377-8398(93)90016-Q

Lermusiaux, P.F.J., Robinson, A.R., 2001. Features of dominant mesoscale variability, circulation patterns and dynamics in the strait of sicily. Deep Sea Res 1 Oceanogr Res Pap 48, 1953–1997. https://doi.org/10.1016/S0967-0637(00)00114-X

Lionello, P., Malanotte-Rizzoli, P., Boscolo, R., Alpert, P., Artale, V., Li, L., Luterbacher, J., May, W., Trigo, R., Tsimplis, M., Ulbrich, U., Xoplaki, E., 2006. The Mediterranean climate: An overview of the main characteristics and issues. Developments in Earth and Environmental Sciences 4, 1–26. https://doi.org/10.1016/S1571-9197(06)80003-0

Lirer, F., Sprovieri, M., Vallefuoco, M., Ferraro, L., Pelosi, N., Giordano, L., Capotondi, L., 2014. Planktonic foraminifera as bio-indicators for monitoring the climatic changes that have occurred over the past 2000 years in the southeastern tyrrhenian sea. Integr Zool 9, 542–554. https://doi.org/10.1111/1749-4877.12083

Lockwood, M., Harrison, R.G., Woollings, T., Solanki, S.K., 2010. Are cold winters in Europe associated with low solar activity? Environmental Research Letters 5, 24001. https://doi.org/10.1088/1748-9326/5/2/024001

Loulergue, L., Schilt, A., Spahni, R., Masson-Delmotte, V., Blunier, T., Lemieux, B., Barnola, J.-M., Raynaud, D., Stocker, T.F., Chappellaz, J., 2008. Orbital and millennial-scale features of atmospheric CH4 over the past 800,000 years. Nature 453, 383–386. https://doi.org/10.1038/nature06950

Lüthi, D., le Floch, M., Bereiter, B., Blunier, T., Barnola, J.-M., Siegenthaler, U., Raynaud, D., Jouzel, J., Fischer, H., Kawamura, K., Stocker, T.F., 2008. High-resolution carbon dioxide concentration record 650,000-800,000 years before present. Nature 453, 379–382. https://doi.org/10.1038/nature06949

Luukko P.J., Helske J., Räsänen E., 2016. Introducing libeemd: A program package for performing the ensemble empirical mode decomposition. Computational Statistics, 31(2), 545–557, doi: 10.1007/s00180-015-0603-9

Malanotte-Rizzoli, P., Artale, V., Borzelli-Eusebi, G.L., Brenner, S., Crise, A., Gacic, M., Kress, N., Marullo, S., Ribera D'Alcalà, M., Sofianos, S., Tanhua, T., Theocharis, A., Alvarez, M., Ashkenazy, Y., Bergamasco, A., Cardin, V., Carniel, S., Civitarese, G., D'Ortenzio, F., Font, J., Garcia-Ladona, E., Garcia-Lafuente, J.M., Gogou, A., Gregoire, M., Hainbucher, D., Kontoyannis, H., Kovacevic, V., Kraskapoulou, E., Kroskos, G., Incarbona, A., Mazzocchi, M.G., Orlic, M., Ozsoy, E., Pascual, A., Poulain, P.-M., Roether, W., Rubino, A., Schroeder, K., Siokou-Frangou, J., Souvermezoglou, E., Sprovieri, M., Tintoré, J., Triantafyllou, G., 2014. Physical forcing and physical/biochemical variability of the Mediterranean Sea: A review of unresolved issues and directions for future research. Ocean Science 10. https://doi.org/10.5194/os-10-281-2014

Malanotte-Rizzoli, P., Hecht, A., 1988. Large-scale properties of the eastern Mediterranean: a review. Oceanologica Acta 11, 323–335. https://doi.org/10.1016/S0967-0645(99)00020-X

Margaritelli, G, Cacho, I., Català, A., Barra, M., Bellucci, L.G., Lubritto, C., Rettori, R., Lirer, F., 2020a. Persistent warm Mediterranean surface waters during the Roman period. Sci Rep 10, 10431. https://doi.org/10.1038/s41598-020-67281-2

Margaritelli, G., Cisneros, M., Cacho, I., Capotondi, L., Vallefuoco, M., Rettori, R., Lirer, F., 2018. Climatic variability over the last 3000 years in the central - western Mediterranean Sea (Menorca Basin) detected by planktonic foraminifera and stable isotope records. Glob Planet Change 169, 179–187. https://doi.org/10.1016/j.gloplacha.2018.07.012

Margaritelli, G., Lirer, F., Schroeder, K., Alberico, I., Dentici, M.P., Caruso, A., 2020b. Globorotalia truncatulinoides in Central - Western Mediterranean Sea during the Little Ice Age. Mar Micropaleontol 161, 101921. https://doi.org/https://doi.org/10.1016/j.marmicro.2020.101921

Margaritelli, G., Vallefuoco, M., di Rita, F., Capotondi, L., Bellucci, L.G., Insinga, D.D., Petrosino, P., Bonomo, S., Cacho, I., Cascella, A., Ferraro, L., Florindo, F., Lubritto, C., Lurcock, P.C., Magri, D., Pelosi, N., Rettori, R., Lirer, F., 2016. Marine response to climate changes during the last five millennia in the central Mediterranean Sea. Glob Planet Change 142, 53–72. https://doi.org/https://doi.org/10.1016/j.gloplacha.2016.04.007

Marriner, N., Kaniewski, D., Pourkerman, M., Devillers, B., 2022. Anthropocene tipping point reverses long-term Holocene cooling of the Mediterranean Sea: A meta-analysis of the basin's

Sea Surface Temperature records. Earth Sci Rev 227, 103986. https://doi.org/https://doi.org/10.1016/j.earscirev.2022.103986

McGregor, H. v., Evans, M.N., Goosse, H., Leduc, G., Martrat, B., Addison, J.A., Mortyn, P.G., Oppo, D.W., Seidenkrantz, M.S., Sicre, M.A., Phipps, S.J., Selvaraj, K., Thirumalai, K., Filipsson, H.L., Ersek, V., 2015. Robust global ocean cooling trend for the pre-industrial Common Era. Nat Geosci 8, 671–677. https://doi.org/10.1038/ngeo2510

McIntyre, A., Molfino, B., 1996. Forcing of Atlantic Equatorial and Subpolar Millennial Cycles by Precession. Science. https://doi.org/10.1126/science.274.5294.1867

MedECC, 2021. Climate and Environmental Change in the Mediterranean Basin – Current Situation and Risks for the Future. First Mediterranean Assessment Report.

Millot, C., 1999. Circulation in the Western Mediterranean Sea. Journal of Marine Systems 20, 423–442. https://doi.org/10.1016/S0924-7963(98)00078-5

Molfino, B., McIntyre, A., 1990. Precessional forcing of nutricline dynamics in the equatorial atlantic. Science 249, 766–769. https://doi.org/10.1126/science.249.4970.766

Moreno, A., Cacho, I., Canals, M., Grimalt, J.O., Sánchez-Goñi, M.F., Shackleton, N., Sierro, F.J., 2005. Links between marine and atmospheric processes oscillating on a millennial time-scale. A multi-proxy study of the last 50,000 yr from the Alboran Sea (Western Mediterranean Sea). Quat Sci Rev 24, 1623–1636. https://doi.org/10.1016/j.quascirev.2004.06.018

Negri, A., Capotondi, L., Keller, J., 1999. Calcareous nannofossils, planktonic foraminifera and oxygen isotopes in the late Quaternary sapropels of the Ionian Sea. Mar Geol 157, 89–103. https://doi.org/10.1016/S0025-3227(98)00135-2

Neukom, R., Steiger, N., Gómez-Navarro, J.J., Wang, J., Werner, J.P., 2019. No evidence for globally coherent warm and cold periods over the preindustrial Common Era. Nature 571, 550–554. https://doi.org/10.1038/s41586-019-1401-2

Olsen, J., Anderson, N.J., Knudsen, M.F., 2012. Variability of the North Atlantic Oscillation over the past 5,200 years. Nat Geosci 5, 808–812. https://doi.org/10.1038/ngeo1589

Oviedo, A., Ziveri, P., Álvarez, M., Tanhua, T., 2015. Is coccolithophore distribution in the Mediterranean Sea related to seawater carbonate chemistry? Ocean Sci 11, 13–32. https://doi.org/10.5194/os-11-13-2015

Pallacks, S., Ziveri, P., Martrat, B., Mortyn, P.G., Grelaud, M., Schiebel, R., Incarbona, A., Garcia-Orellana, J., Anglada-Ortiz, G., 2021. Planktic foraminiferal changes in the western Mediterranean Anthropocene. Glob Planet Change 204, 103549. https://doi.org/https://doi.org/10.1016/j.gloplacha.2021.103549

Pinardi, N., Masetti, E., 2000. Variability of the large scale general circulation of the Mediterranean Sea from observations and modelling: A review. Palaeogeogr Palaeoclimatol Palaeoecol 158, 153–174. https://doi.org/10.1016/S0031-0182(00)00048-1

Rigual-Hernández, A.S., Bárcena, M.A., Jordan, R.W., Sierro, F.J., Flores, J.A., Meier, K.J.S., Beaufort, L., Heussner, S., 2013. Diatom fluxes in the NW Mediterranean: Evidence from a 12-year sediment trap record and surficial sediments. J Plankton Res 35, 1109–1125. https://doi.org/10.1093/plankt/fbt055

Rigual-Hernández, A.S., Sierro, F.J., Bárcena, M.A., Flores, J.A., Heussner, S., 2012. Seasonal and interannual changes of planktic foraminiferal fluxes in the Gulf of Lions (NW Mediterranean) and their implications for paleoceanographic studies: Two 12-year sediment trap records. Deep Sea Research Part I: Oceanographic Research Papers 66, 26–40. https://doi.org/https://doi.org/10.1016/j.dsr.2012.03.011

Robinson, A.R., Golnaraghi, M., 1994. The physical and dynamical oceanography of the Mediterranean Sea, in: Ocean Processes in Climate Dynamics: Global and Mediterranean Examples. pp. 255–306. https://doi.org/10.1007/978-94-011-0870-6_12

Robinson, A.R., Sellschopp, J., Warn-Varnas, A., Leslie, W.G., Lozano, C.J., Haley, P.J., Anderson, L. a., Lermusiaux, P.F.J., 1999. The Atlantic Ionian stream. Journal of Marine Systems 20, 129–156. https://doi.org/10.1016/S0924-7963(98)00079-7

Roesch, A., and Schmidbauer H., 2014. WaveletComp 1.0: A guided tour through the R-package. https://doi.org/10.13140/RG.2.2.26317.44009

Rohling, E.J., Marino, G., Grant, K.M., 2015. Mediterranean climate and oceanography, and the periodic development of anoxic events (sapropels). Earth Sci Rev 143, 62–97. https://doi.org/10.1016/j.earscirev.2015.01.008

Rutten, a., de Lange, G.J., Ziveri, P., Thomson, J., van Santvoort, P.J.M., Colley, S., Corselli, C., 2000. Recent terrestrial and carbonate fluxes in the pelagic eastern Mediterranean; a comparison between sediment trap and surface sediment. Palaeogeogr Palaeoclimatol Palaeoecol 158, 197–213. https://doi.org/10.1016/S0031-0182(00)00050-X

Seyfried, L., Estournel, C., Marsaleix, P., Richard, E., 2019. Dynamics of the North Balearic Front during an autumn tramontane and mistral storm: air–sea coupling processes and stratification budget diagnostic. Ocean Science 15, 179–198. https://doi.org/10.5194/os-15-179-2019

Siegenthaler, U., Monnin, E., Kawamura, K., Spahni, R., Schwander, J., Stauffer, B., Stocker, T.F., Barnola, J., Fischer, H., 2005. Supporting evidence from the EPICA Dronning Maud Land ice core for atmospheric CO 2 changes during the past millennium. Tellus 57B, 51–57.

Sirocko, F., Brunck, H., Pfahl, S., 2012. Solar influence on winter severity in central Europe. Geophys Res Lett 39. https://doi.org/https://doi.org/10.1029/2012GL052412

Smith, A.C., Wynn, P.M., Barker, P.A., Leng, M.J., Noble, S.R., Tych, W., 2016. North Atlantic forcing of moisture delivery to Europe throughout the Holocene. Sci Rep 6, 1–7. https://doi.org/10.1038/srep24745

Soon, W., Velasco Herrera, V.M., Selvaraj, K., Traversi, R., Usoskin, I., Chen, C.-T.A., Lou, J.-Y., Kao, S.-J., Carter, R.M., Pipin, V., Severi, M., Becagli, S., 2014. A review of Holocene solar-linked climatic variation on centennial to millennial timescales: Physical processes, interpretative frameworks and a new multiple cross-wavelet transform algorithm. Earth Sci Rev 134, 1–15. https://doi.org/https://doi.org/10.1016/j.earscirev.2014.03.003

Steinhilber, F., Beer, J., Fröhlich, C., 2009. Total solar irradiance during the Holocene. Geophys Res Lett 36. https://doi.org/https://doi.org/10.1029/2009GL040142

Triantaphyllou, M.V., 2014. Coccolithophore assemblages during the Holocene Climatic Optimum in the NE Mediterranean (Aegean and northern Levantine Seas, Greece): Paleoceanographic and paleoclimatic implications. Quaternary International. https://doi.org/10.1016/j.quaint.2014.01.033

Triantaphyllou, M.V., Antonarakou, A., Kouli, K., Dimiza, M.D., Kontakiotis, G., Papanikolaou, M.D., Ziveri, P., Mortyn, P.G., Lianou, V., Lykousis, V., Dermitzakis, M.D., 2009. Late Glacial-Holocene ecostratigraphy of the south-eastern Aegean Sea, based on plankton and pollen assemblages. Geo-Marine Letters 29, 249–267. https://doi.org/10.1007/s00367-009-0139-5

Triantaphyllou, M.V., Ziveri, P., Gogou, A., Marino, G., Lykousis, V., Bouloubassi, I., Emeis, K.C., Kouli, K., Dimiza, M.D., Rosell-Melé, A., Papanikolaou, M., Katsouras, G., Nunez, N., 2009. Late Glacial-Holocene climate variability at the south-eastern margin of the Aegean Sea. Mar Geol 266, 182–197. https://doi.org/10.1016/j.margeo.2009.08.005

Triantaphyllou, M.V., Ziveri, P., Tselepides, A., 2004. Coccolithophore export production and response to seasonal surface water variability in the oligotrophic Cretan Sea (NE Mediterranean). Micropaleontology 50, 127–144.

Trouet, V.J.N.E.B.A.J.D.F.D.C., 2009. Persistent Positive North Atlantic Oscillation Mode Dominated the Medieval Climate Anomaly. Science (1979) 324, 78–80.

Vallefuoco, M., Lirer, F., Ferraro, L., Pelosi, N., Capotondi, L., Sprovieri, M., Incarbona, A., 2012. Climatic variability and anthropogenic signatures in the Gulf of Salerno (southern-eastern Tyrrhenian Sea) during the last half millennium. Rendiconti Lincei 23, 13–23. https://doi.org/10.1007/s12210-011-0154-0

Wu Z., Huang N.E., 2009. Ensemble empirical mode decomposition: a noise-assisted data analysis method. Adv. Adapt. Data Anal., 01, 1–41.
Young, J.R., 1994. Functions of coccoliths, in: Winter, A., Siesser, W.G. (Eds.), Coccolithophores. Cambridge Univ. Press, Cambridge, pp. 63–82.
Young, J.R., Geisen, M., Cros, L., Kleijne, A., Sprengel, C., Probert, I., Østergaard, J., 2003. A guide to extant coccolithophore taxonomy. Journal of Nannoplankton Research 125.
Ziveri, P., Rutten, A., de Lange, G.J., Thomson, J., Corselli, C., 2000. Present-day coccolith fluxes recorded in central eastern Mediterranean sediment traps and surface sediments. Palaeogeogr Palaeoclimatol Palaeoecol 158, 175–195. https://doi.org/10.1016/S0031-0182(00)00049-3

Captions

Figure 1: Bathymetric map of the western Mediterranean Sea (Ocean Data View software), location map of MR-3.3 core (blue circle) and oceanographic features modified from Millot et al. (1999), Pinardi and Masetti (2000) and Seyfried et al. (2019). Black arrows show the MAW path: AC, Algerian Current; LG, Lions Gyre; deep-water formation site; LPCC, Liguro-Provençe-Catalan Current. Black dotted arrows show meso-scale eddies from AC instability. White circles, location of: 1, Nmin 1 and 2 cores (Cisneros et al., 2019); 2, Mallorca speleothems (Cisneros et al., 2021); 3, Cava de Asiul speleothems (Smith et al., 2016). White and yellow stars respectively show stations of the coccolithophore surveys VICOMED I and II.

Figure 2: Downcore variations of selected coccolith taxa (%) and coccolith diversity index (Shannon-Wiener H-Index) in core MR-3.3, plotted *versus* age expressed in years CE. Black horizontal bars show the error associated to countings for a 95% confidence level. Thick black lines represent the 3-pt running average. Grey and white boxes show preindustrial changes in climate and society, drawn following Buntgen et al. (2016), Margaritelli et al. (2018) and Neukom et al. (2019). TP: Talaiotic Period; RP: Roman Period; Dark Age; LA LIA: Late Antique Little Ice Age; MCA: Medieval Climate Anomaly; LIA: Little Ice Age.

Figure 3: Downcore variations of coccolith groups (%) in core MR-3.3, plotted *versus* age expressed in years CE. Black horizontal bars show the error associated to countings for a 95% confidence level. Thick black lines represent the 3-pt running average. Grey and white boxes show preindustrial changes in climate and society, drawn following Buntgen et al. (2016),

Margaritelli et al. (2018) and Neukom et al. (2019). TP: Talaiotic Period; RP: Roman Period; Dark Age; LA LIA: Late Antique Little Ice Age; MCA: Medieval Climate Anomaly; LIA: Little Ice Age.

Figure 4: scatter plots of coccolith groups (%) in core MR-3.3, whose correlation is significant adopting results from the T-student test (see Tab. 1). *Florisphaera profunda* equals LPZ group. The black line shows the linear fit. The equation of the linear fit, R^2 correlation index and number of samples are also reported.

Figure 5: Downcore variations of selected coccolith taxa (%) in core MR-3.3, plotted *versus* age expressed in years CE, in comparison with climatic and oceanographic proxies. A: coccolith N-Ratio in core MR-3.3 (this study), as a proxy of the nutricline depth. The thick black line shows the linear trend. B: Total Solar Irradiation (W/m^2) (Steinhilber et al., 2009). The thick red curve represents the 3-pt running average. The red filling shows values lower than -0.2 of solar minima. C: *Globigerinoides ruber* $\delta^{18}O$ (‰) in core MR-3.3 (Margaritelli et al., 2018). D: *Globigerina bulloides* Mg/Ca SST (°C) in core MR-3.3 (Cisneros et al., 2016). E: Mediterranean SST (°C) stack (Martinez et al., 2022). The thick green curve represents the 15-pt running average. F: *Emiliania huxleyi* (%) in core MR-3.3 (this study). Note the reverse axis. The brown filling shows values higher than 1.0%. G: the sum of *Turborotalita quinqueloba* and *Globigerinita glutinata* (%) in core MR-3.3 (Margaritelli et al., 2018), as a proxy of surface water productivity. The thick grey curve represents the 3-pt running average. The thick grey line shows the linear trend. H: the sum of *Neogloboquadrina incompta* and *Neogloboquadrina dutertrei* (%) in core MR-3.3 (Margaritelli et al., 2018), as a proxy of deep chlorophyll maximum. The thick purple curve represents the 3-pt running average. The thick purple line shows the linear trend. Grey and white boxes show preindustrial changes in climate and society, drawn following Buntgen et al. (2016), Margaritelli et al. (2018) and Neukom et al. (2019). TP: Talaiotic Period; RP: Roman Period; Dark Age; LA LIA: Late Antique Little Ice Age; MCA: Medieval Climate Anomaly; LIA: Little Ice Age.

Figure 6: Spectral analysis of *Florisphaera profunda* data in core MR-3.3 and comparison with TSI. A: Bias-corrected power spectrum of unevenly sampled *F. profunda* abundance. Red and green lines respectively refer to 99 and 95% confidence level. Significant periodicities are indicated. B: Cross-wavelet analysis between *F. profunda* percentage values in core MR-3.3 and TSI (Steinhilber et al., 2009) throughout the last 2700 years of the record (years in CE). C:

IMF5 of *F. profunda* percentage values in core MR-3.3 and TSI (Steinhilber et al., 2009) throughout the last 2700 years of the record (years in CE). Grey and white boxes show preindustrial changes in climate and society, drawn following Buntgen et al. (2016), Margaritelli et al. (2018) and Neukom et al. (2019). TP: Talaiotic Period; RP: Roman Period; Dark Age; LA LIA: Late Antique Little Ice Age; MCA: Medieval Climate Anomaly; LIA: Little Ice Age. D: Cross-correlation analysis between *F. profunda* percentage values in core MR-3.3 and TSI (Steinhilber et al., 2009) throughout the last 2700 years of the record.

Figure 7: Downcore variations of holococcoliths (%) in core MR-3.3, plotted *versus* age expressed in years CE, in comparison with climatic and oceanographic proxies. A: holococcoliths in core MR-3.3 (this study), as a proxy of seafloor ventilation. Note the reverse axis. The black filling shows values higher than 1.5%. B: C26OH (%) Index Aegean Sea (Gogou et al., 2016). The grey filling shows values lower than 30.0%. C: non-cohesive silt fraction (UP10) percentage values from NMin1 (red curve) and NMin2 (blue curve) Balearic Sea cores (Fig. 1) (Cisneros et al., 2019). Red (= 42.5%) and blue (37.5%) fillings refer to numerical sills that would determine deepwater formation events. D: $\delta^{18}O$ (‰) from Cueva de Asiul speleothems, North Spain (Fig. 1) (Smith et al., 2016). The brown filling shows values lower than 0.0‰. The black dashed refers to detrended data. E: $\delta^{18}O$ Mallorca speleothem composite record (Fig. 1) (Cisneros et al., 2021). The green filling shows values lower than 0.0‰. F: NAO reconstructions (Trouet et al., 2009, blue line; Olsen et al., 2012, orange line; Faust et al., 2016, light green line). The three curves represent a 5-pt running average. G: *Globigerina bulloides* $\delta^{18}O_{seawater}$ in core MR-3.3 (Cisneros et al., 2016). The purple curve represents a 3-pt running average. Grey and white boxes show preindustrial changes in climate and society, drawn following Buntgen et al. (2016), Margaritelli et al. (2018) and Neukom et al. (2019). TP: Talaiotic Period; RP: Roman Period; Dark Age; LA LIA: Late Antique Little Ice Age; MCA: Medieval Climate Anomaly; LIA: Little Ice Age.

Table 1: results from the T-student test for coccolith groups. In red, R values. In Blue, p values. In bold, statistically significant results ($p < 0.005$).

Supplementary Data Table 1: raw and percentage data of coccolith taxa. Ehux<4: *Emiliania huxleyi* < 4µm. Ehux>4: *Emiliania huxleyi* > 4µm. smg: small *Gephyrocapsa*. Gmue: *Gephyrocapsa muellerae*. Goc: *Gephyrocapsa oceanica*. Gcar: *Gephyrocapsa caribbeanica*. Spul: *Syracosphaera pulchra*. Umbello: *Umbellosphaera* spp.. Dtub: *Discosphaera tubifera.*

Rhab: *Rhabdosphaera* spp.. Umbilico: *Umbilicosphaera sibogae*. Oolit: *Oolithotus fragilis*. Calcio: *Calciosolenia* spp.. Holo: holococcoliths. Cerat: *Ceratolithus cristatus.* Thei: *Thoracosphaera heimii.* Hspp: *Helicosphaera* spp.. Hcar: *Helicosphaera carteri.* Hwal: *Helicosphaera wallichii.* Hpav: *Helicosphaera pavimentum.* Cpel: *Coccolithus pelagicus pelagicus.* Cbra: *Coccolithus pelagicus braarudii.* Shis: *Syracosphaera histrica.* Pont: *Pontosphaera* spp.. Clep: *Calcidiscus leptoporus.* Corono: *Coronosphaera* spp.. Bbig: *Braarudosphaera bigelowii.* Others: specimens of all other species. Fprof: *Florisphaera profunda.* Reworked: reworked specimens.

Journal Pre-proof

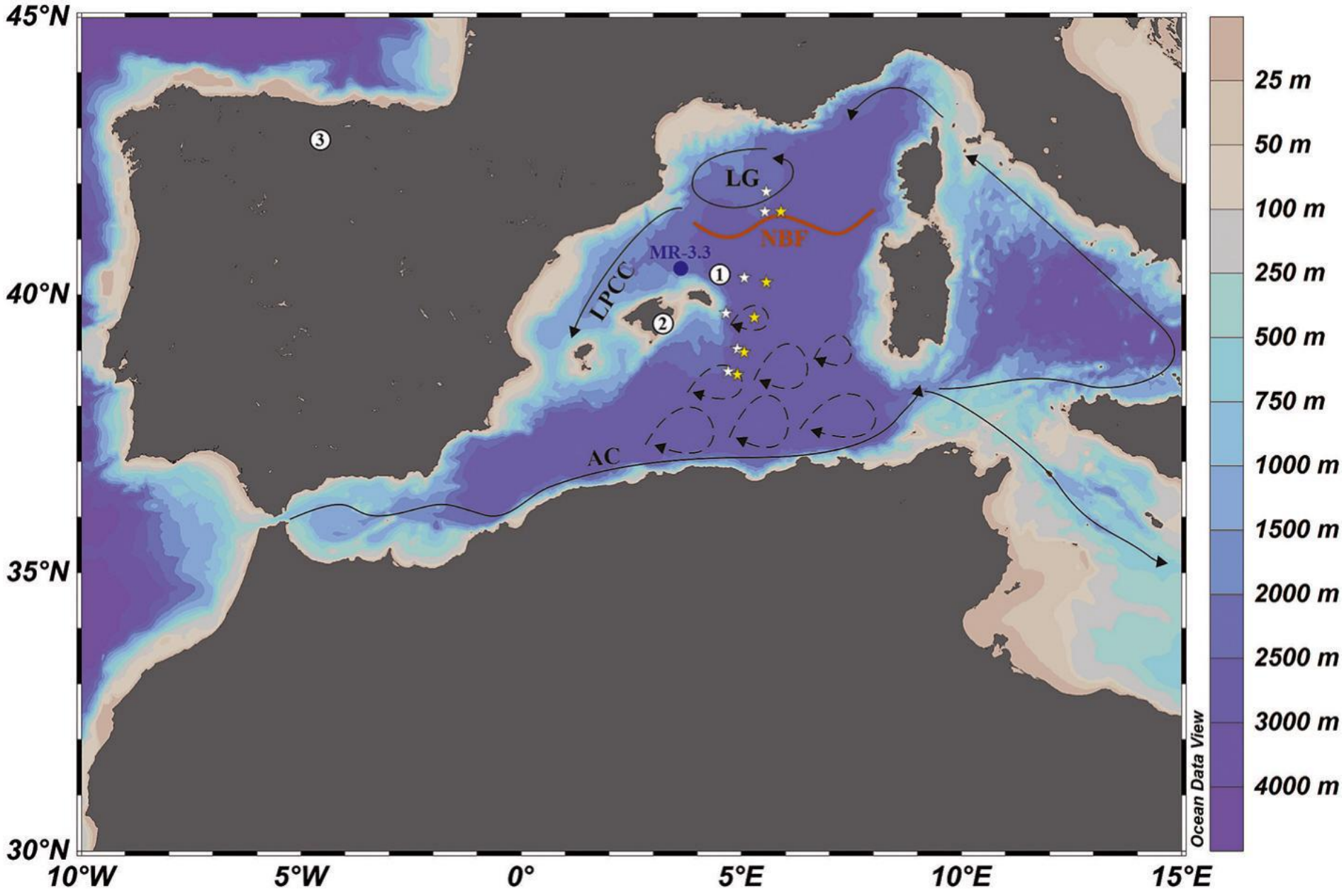
45°N
40°N
35°N
30°N
10°W
5°W
0°
5°E
10°E
15°E
LG
NBF
MR-3.3
LPCC
AC
1
2
3
25 m
50 m
100 m
250 m
500 m
750 m
1000 m
1500 m
2000 m
2500 m
3000 m
4000 m
Ocean Data View

Figure 1

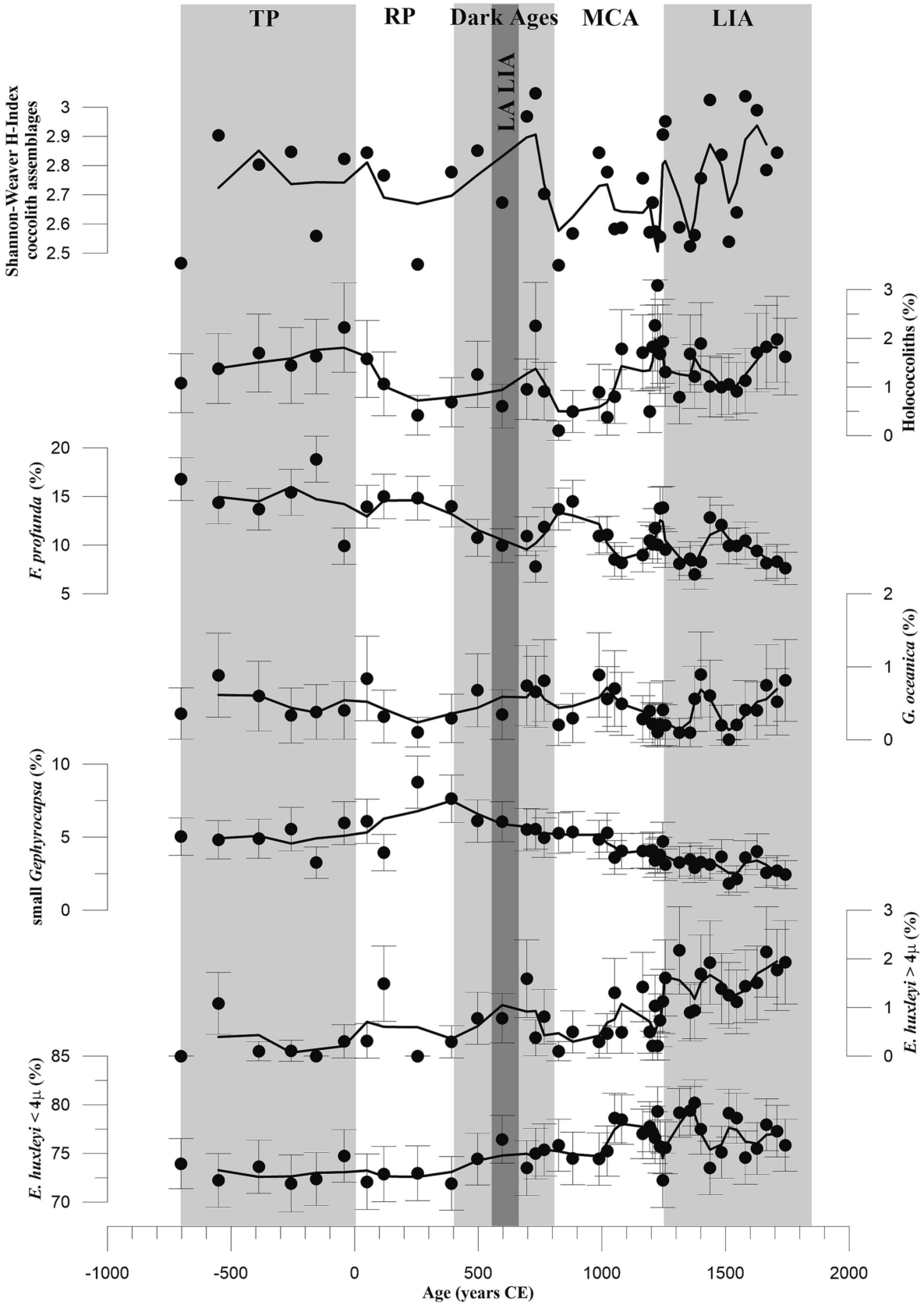
TP
RP
Dark Ages
MCA
LIA
LA LIA
Shannon-Weaver H-Index coccolith assemblages
3
2.9
2.8
2.7
2.6
2.5
Holococcoliths (%)
3
2
1
0
F. profunda (%)
20
15
10
5
G. oceanica (%)
2
1
0
small Gephyrocapsa (%)
10
5
0
E. huxleyi > 4μ (%)
3
2
1
0
E. huxleyi < 4μ (%)
85
80
75
70
-1000
-500
0
500
1000
1500
2000
Age (years CE)

Figure 2

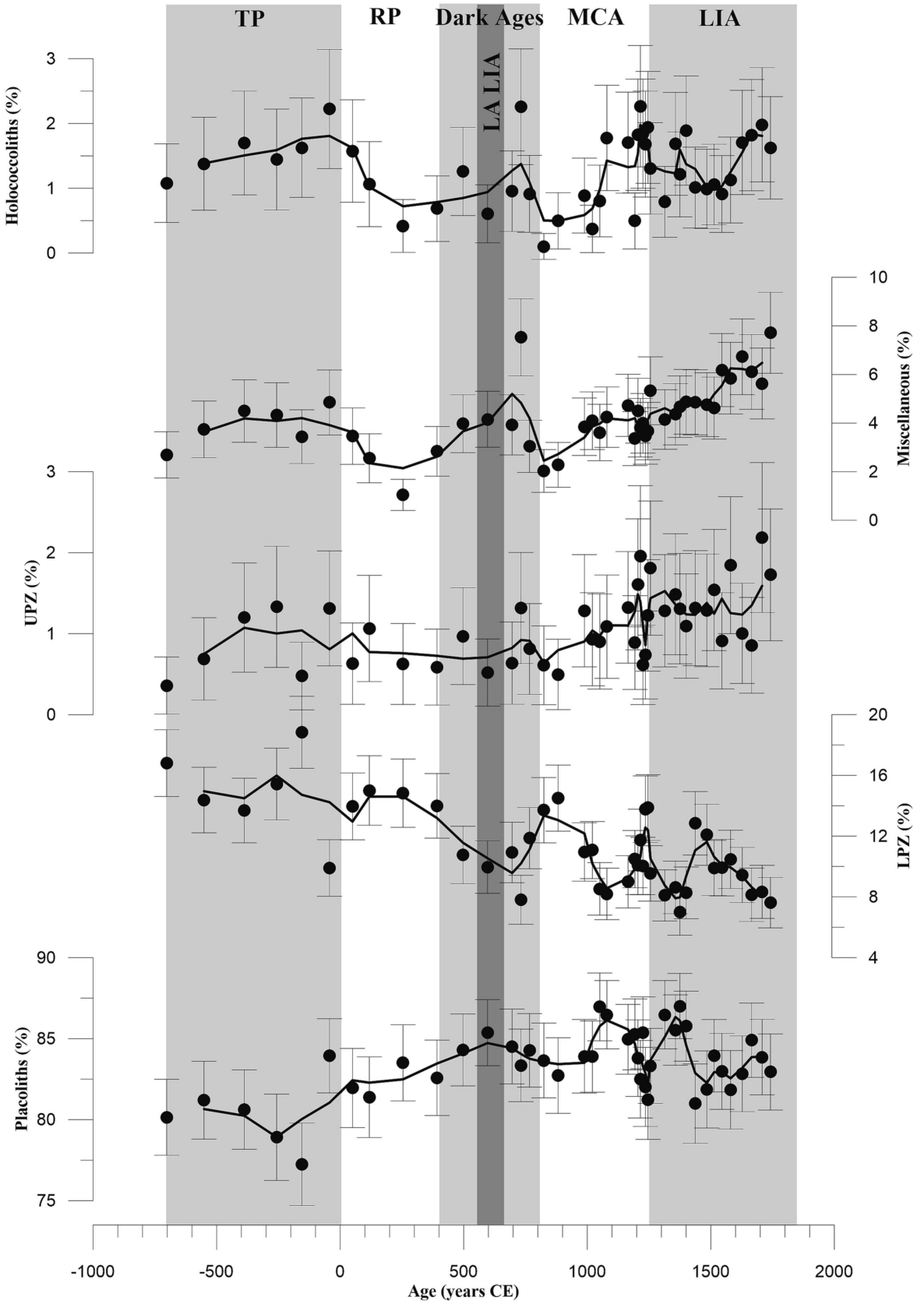
TP
RP
Dark Ages
MCA
LIA
LA LIA
Holococcoliths (%)
Miscellaneous (%)
UPZ (%)
LPZ (%)
Placoliths (%)
Age (years CE)
-1000
-500
0
500
1000
1500
2000

Figure 3

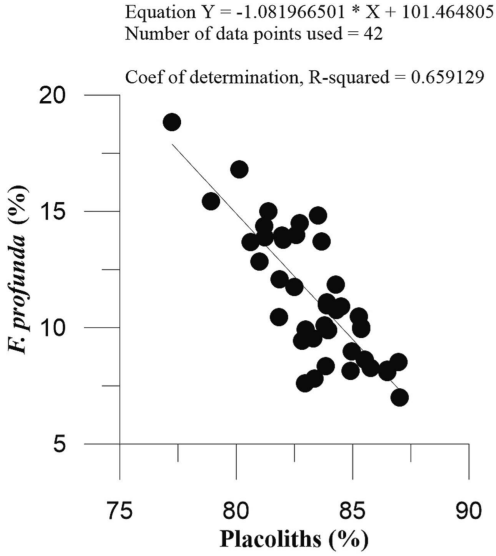
Equation Y = -1.081966501 * X + 101.464805
Number of data points used = 42
Coef of determination, R-squared = 0.659129
F. profunda (%)
Placoliths (%)

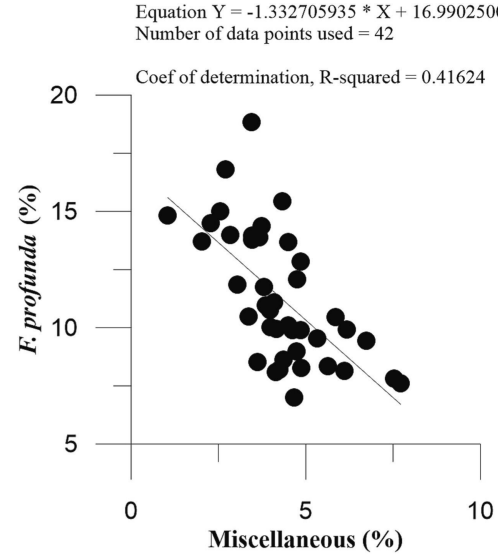
Equation Y = -1.332705935 * X + 16.99025003
Number of data points used = 42
Coef of determination, R-squared = 0.41624
F. profunda (%)
Miscellaneous (%)

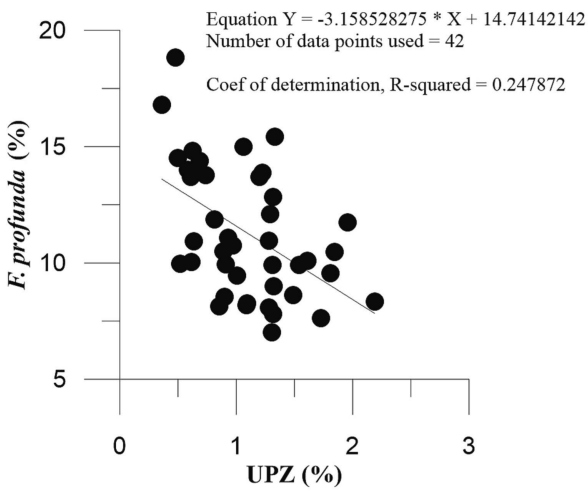
Equation Y = -3.158528275 * X + 14.74142142
Number of data points used = 42
Coef of determination, R-squared = 0.247872
F. profunda (%)
UPZ (%)

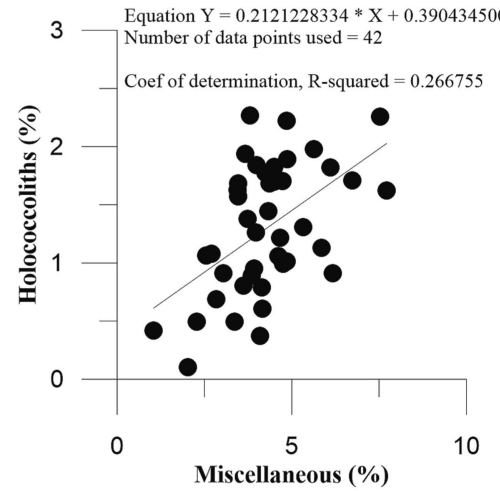
Equation Y = 0.2121228334 * X + 0.3904345001
Number of data points used = 42
Coef of determination, R-squared = 0.266755
Holococcoliths (%)
Miscellaneous (%)

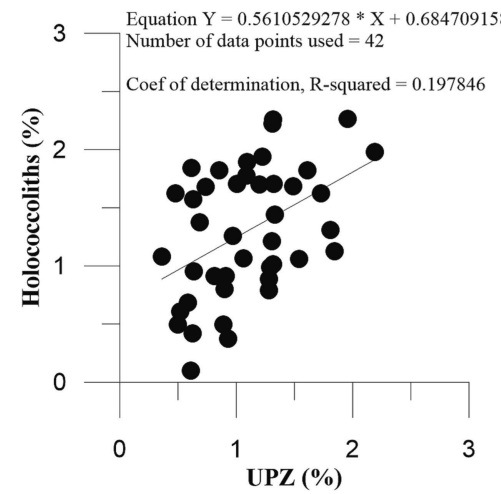
Equation Y = 0.5610529278 * X + 0.684709158
Number of data points used = 42
Coef of determination, R-squared = 0.197846
Holococcoliths (%)
UPZ (%)

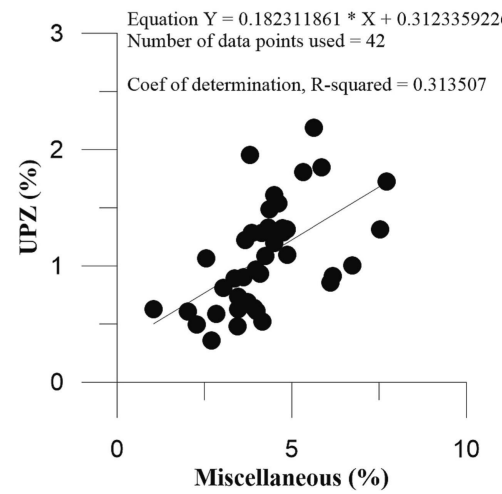
Equation Y = 0.182311861 * X + 0.3123359226
Number of data points used = 42
Coef of determination, R-squared = 0.313507
UPZ (%)
Miscellaneous (%)

Figure 4

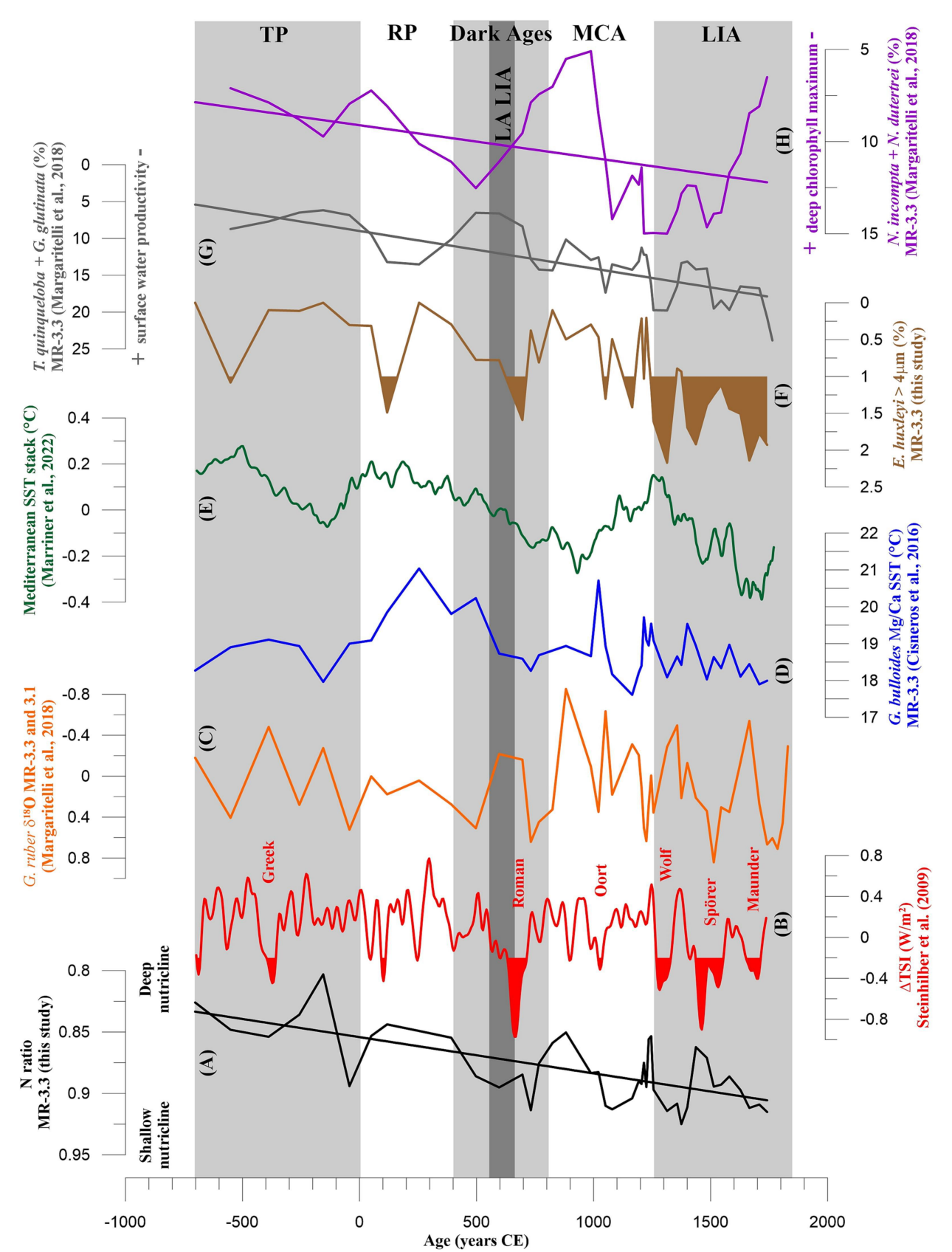
TP
RP
Dark Ages
MCA
LIA
LA LIA
(A)
(B)
(C)
(D)
(E)
(F)
(G)
(H)
Greek
Roman
Oort
Wolf
Spörer
Maunder
N ratio
MR-3.3 (this study)
Deep nutricline
Shallow nutricline
G. ruber δ18O MR-3.3 and 3.1
(Margaritelli et al., 2018)
ΔTSI (W/m2)
Steinhilber et al. (2009)
Mediterranean SST stack (°C)
(Marriner et al., 2022)
G. bulloides Mg/Ca SST (°C)
MR-3.3 (Cisneros et al., 2016)
E. huxleyi > 4μm (%)
MR-3.3 (this study)
T. quinqueloba + G. glutinata (%)
MR-3.3 (Margaritelli et al., 2018)
+ surface water productivity -
+ deep chlorophyll maximum -
N. incompta + N. dutertrei (%)
MR-3.3 (Margaritelli et al., 2018)
Age (years CE)

Figure 5

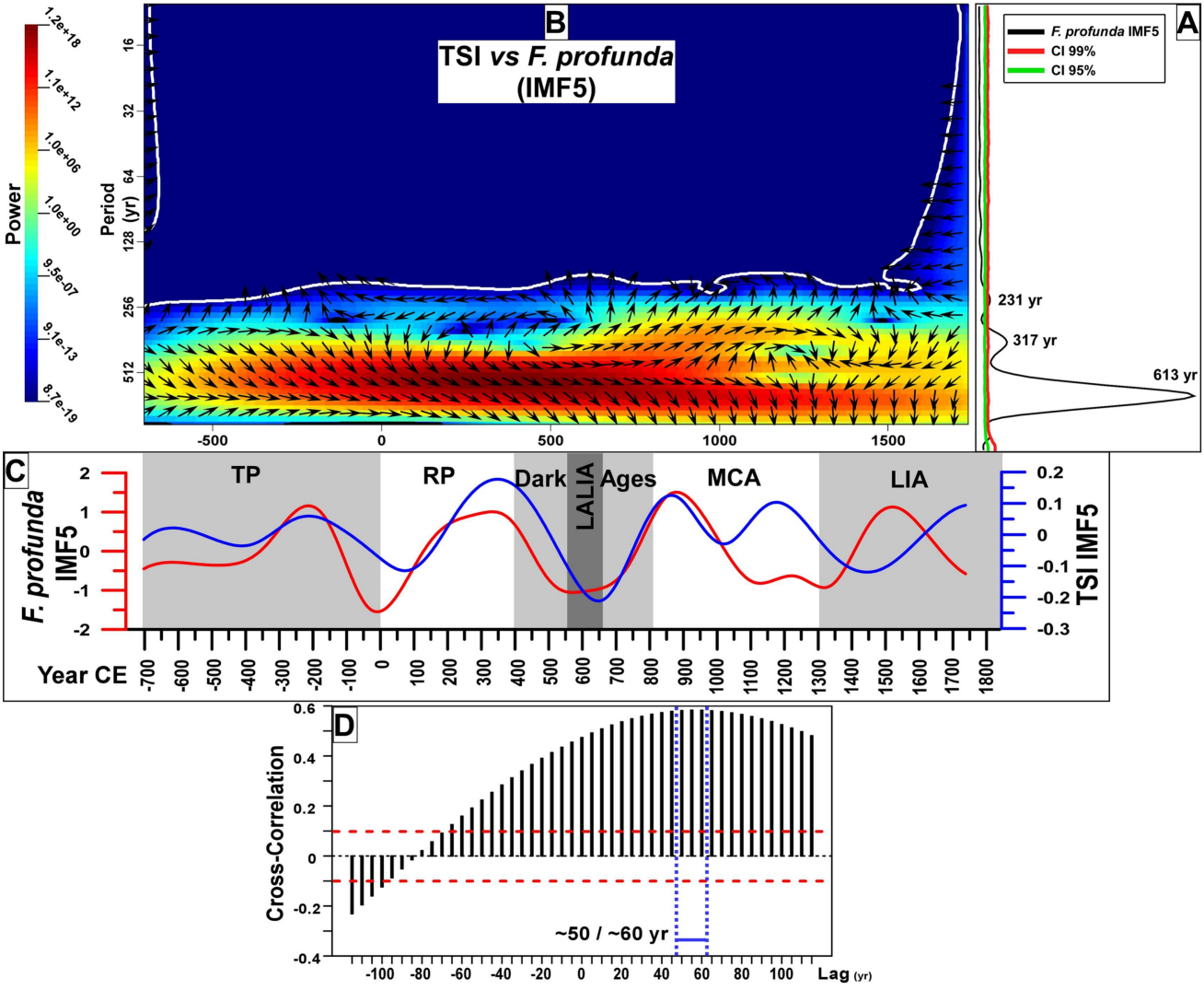
B
TSI vs F. profunda
(IMF5)
Power
1.2e+18
1.1e+12
1.0e+06
1.0e+00
9.5e-07
9.1e-13
8.7e-19
Period (yr)
16
32
64
128
256
512
-500
0
500
1000
1500
A
F. profunda IMF5
CI 99%
CI 95%
231 yr
317 yr
613 yr
C
F. profunda IMF5
TSI IMF5
TP
RP
Dark Ages
LALIA
MCA
LIA
Year CE
D
Cross-Correlation
~50 / ~60 yr
Lag (yr)

Figure 6

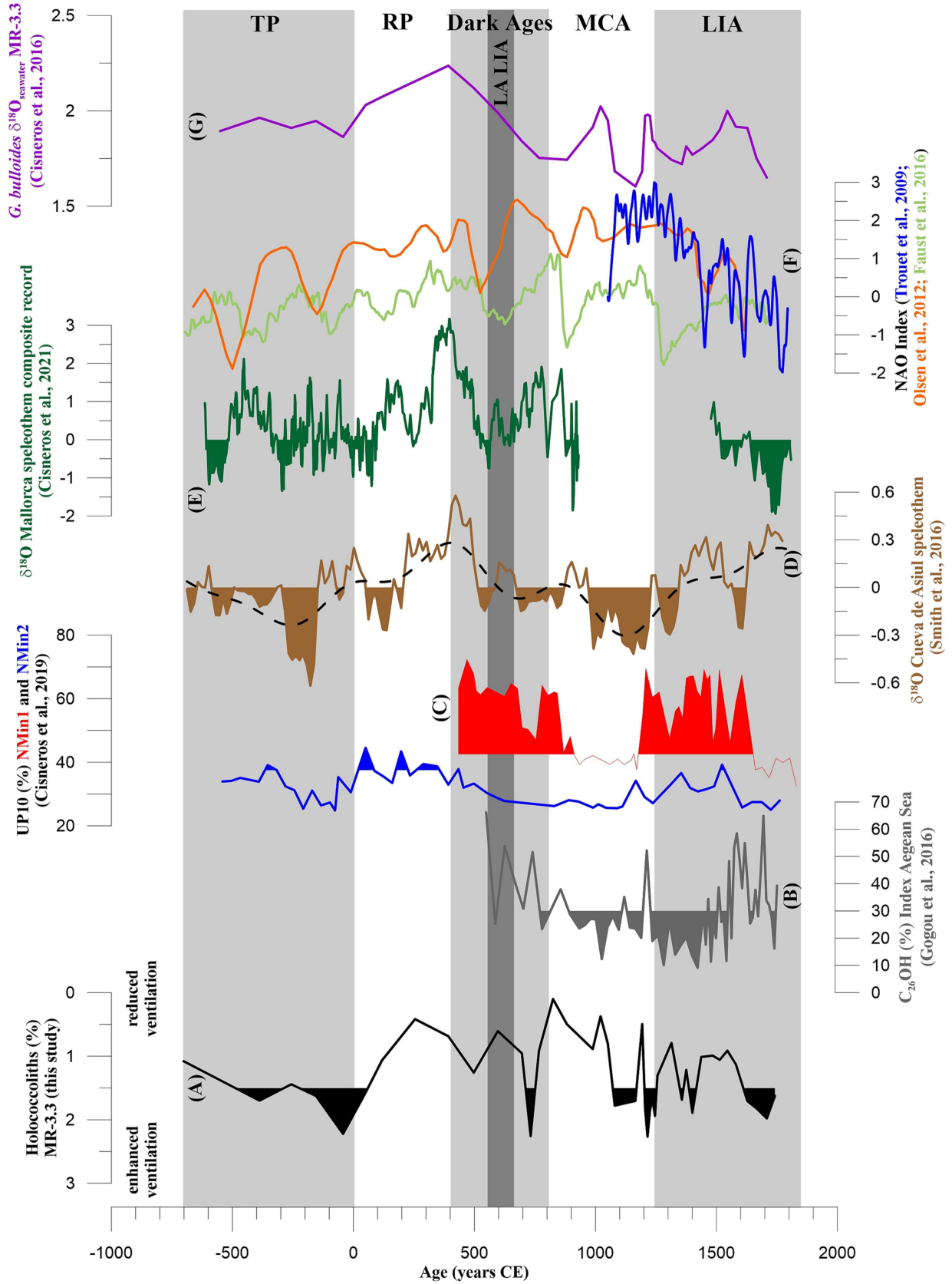
TP
RP
Dark Ages
MCA
LIA
LA LIA
(G)
(F)
(E)
(D)
(C)
(B)
(A)
G. bulloides δ18Oseawater MR-3.3 (Cisneros et al., 2016)
NAO Index (Trouet et al., 2009; Olsen et al., 2012; Faust et al., 2016)
δ18O Mallorca speleothem composite record (Cisneros et al., 2021)
δ18O Cueva de Asiul speleothem (Smith et al., 2016)
UP10 (%) NMin1 and NMin2 (Cisneros et al., 2019)
C26OH (%) Index Aegean Sea (Gogou et al., 2016)
Holococcoliths (%) MR-3.3 (this study)
reduced ventilation
enhanced ventilation
Age (years CE)

Figure 7